

UNIVERSIDADE DE LISBOA  
FACULDADE DE CIÊNCIAS  
DEPARTAMENTO DE BIOLOGIA VEGETAL



**Metabolic remodeling of endothelial cells upon hypoxia  
and  $\beta$ -blockers as anti-angiogenic drugs**

Filipa Alexandra Dias Martins

**Mestrado em Biologia Molecular e Genética**

Dissertação orientada por:

Prof.<sup>a</sup> Doutora Jacinta Serpa  
Prof. Doutor Francisco Dionísio

## Agradecimentos

Terminada esta que foi a fase mais exigente da minha vida académica, não poderia deixar de agradecer a todos os que me apoiaram e que sem dúvida me ajudaram a realizar este trabalho. A eles se dirige este texto.

Em primeiro lugar agradeço à Prof.<sup>a</sup> Doutora Jacinta Serpa por me ter dado a oportunidade de integrar o seu grupo de investigação com um projeto que tanto gozo me deu. Muito obrigada por toda a dedicação, exigência, incentivo ao pensamento crítico e por todos os ensinamentos transmitidos ao longo deste ano. Um especial obrigada por toda a paciência e apoio dado nesta última fase.

Agradeço também ao Prof. Doutor Francisco Dionísio por ter aceite tornar-se meu orientador interno já numa fase tão tardia.

Um obrigada ao Doutor Luís Gafeira por me ter introduzido no universo do NMR e por me ter dado umas luzes quanto à sua análise. Obrigada por toda a disponibilidade e simpatia.

Não poderia deixar de agradecer à Doutora Sílvia Conde que tão amavelmente nos cedeu as aortas que se tornaram indispensáveis para este trabalho.

Agradeço também aos meus colegas do CMM, que tão bem me integraram. Muito obrigada à Cindy, por toda a amizade, pelos desabafos no comboio e por ter sempre um sorriso a dar. À Ana, uma das “aorta girls”, por toda a boa disposição, toda a cantoria e gargalhadas que não foram poucas. Ao Cristiano, por ser uma das pessoas mais inteligentes e divertidas que conheço. À Rakhi por todas as conversas, apoio e por tanto me ter ensinado acerca da sua cultura. À Adriana por me relembrar a minha veia bioquímica com um toque a Aveiro. Ao Donato por toda a simpatia e pelos belos cozinhados italianos. Graças a vocês houve sempre um bom ambiente. Com todos aprendi coisas novas, porém tenho que fazer um agradecimento especial à Filipa Coelho, a rainha das “aorta girls”, que me acolheu “debaixo da sua asa” e com quem muito aprendi. Muito obrigada por todo o apoio, incentivo, amizade e por toda a paciência! Acredito que por vezes não tenha sido fácil!

Agradeço também toda a simpatia e apoio de todos os colegas da UIPM, desde os mais novinhos aos com mais experiência, que tornaram esta experiência muito agradável.

Um especial agradecimento aos meus amigos, por estarem sempre ao meu lado e tanto me apoiarem nesta jornada, por todo o incentivo, pela paciência na hora dos desabafos, pela partilha de histórias e principalmente por me ajudarem a distrair quando mais necessitava.

Por último, mas não menos importante, agradeço aos meus pais e ao meu irmão, por acreditarem em mim, por me inspirarem e por todo o apoio, todos os conselhos, todos os abraços e todos os sorrisos partilhados.

## Abstract

Angiogenesis occurs when new blood vessels sprout from pre-existing ones through proliferation of endothelial cells (ECs). This process plays a major role in several physiological and pathophysiological processes, including atherosclerosis, chronic inflammation and cancer. The tumor-associated neovasculature is responsible for the supply of nutrients and oxygen, promoting tumor growth and metastasis, even though these blood vessels are structurally and functionally abnormal. During tumor progression, rapid and uncontrolled proliferation of tumor cells occurs, leading to a hypoxic microenvironment with insufficient blood supply. Therefore, tumor cells start to release pro-angiogenic factors, such as VEGF (vascular endothelial growth factor), and hypoxia leads to the stabilization of HIF-1 $\alpha$  (hypoxia-inducible factor 1  $\alpha$ ), inducing the expression of genes that will stimulate the formation of a new vessel.

The first objective of this thesis was to unravel the hypoxia effect in metabolic remodeling during the endothelial cell activation. An NMR (nuclear magnetic resonance) analysis of HUVECs (human umbilical vein endothelial cells) exposed to CoCl<sub>2</sub>-mimicked hypoxia showed decreased lactate and 2-hydroxyisobutyrate extracellular levels in hypoxia. In addition, an increase of intracellular formate levels was detected in hypoxia, which suggests a proliferating phenotype due to formate involvement in purine synthesis. On the other hand, there was a decrease in the intracellular levels of glucose, lactate and acetate upon exposure to hypoxia, precursors of pyruvate. Concerning endothelial activation upon hypoxia, an *in vitro* tube forming assay was performed and indicated a promotion of vessel-like structures formation by hypoxia. However, in an *ex vivo* rat aortic ring assay the exposition to CoCl<sub>2</sub> resulted in sprouting inhibition. Besides, a wound healing assay demonstrated a migration inhibition on cells exposed to CoCl<sub>2</sub>. This makes us wonder if the concentration of CoCl<sub>2</sub> used is actually mimicking hypoxia.

Cysteine (Cys) is an important ROS (reactive oxygen species) scavenger, showed to have an involvement in cancer cell remodeling. Since ROS act as pro-angiogenic molecules, we had the intent to investigate the effect of Cys in endothelial activation. An aortic ring assay showed a tendency for a sprouting increase when exposed to Cys and higher branch points density when exposed to H<sub>2</sub>O<sub>2</sub>. However, these levels decreased when exposed to Cys and H<sub>2</sub>O<sub>2</sub>, what suggests that ROS may play a role in inducing angiogenesis, being Cys able to somehow revert this process.

Many anti-angiogenic strategies were developed over the years, but they have failed mostly because the mechanisms involved in neoangiogenesis are not fully understood. Propranolol (a non-selective  $\beta$ -blocker) has emerged as an effective treatment for infantile hemangiomas, leading to its regression. Hence, our second objective was to determine the effect of propranolol in neo-angiogenesis. A tube forming assay was performed and showed that propranolol inhibited the formation and destroyed the already formed vessel-like structures. Its inhibitory effects extended to migration, without affecting cell viability. Besides, an immunofluorescence assay showed that propranolol affected the expression of some EC markers, particularly when the exposure was shorter. The effect was also accessed *ex vivo*, in which propranolol inhibited the sprout of endothelial cells from the aortic ring, corroborating the *in vitro* results.

The metabolic remodeling involved during aortic ring sprouting was also accessed by NMR spectroscopy, showing the differential expression of metabolites from different pathways, glycolysis, aminoacyl-tRNA biosynthesis, valine, leucine and isoleucine biosynthesis and degradation.

This study gives some insights into the metabolic remodeling induced by hypoxia in endothelial cells, opening new cues on the metabolic adaptation underlying angiogenesis which, despite being a process involving non-cancerous cells it accounts for cancer progression. The results on the effect of propranolol in angiogenesis reinforces its use as a therapeutic alternative to target angiogenesis and treat cancer not only vascular tumors, being a starting point to further investigations on the mechanisms underlying its action.

**Keywords:** Endothelial cells; Angiogenesis; Tumor microenvironment; Hypoxia; Propranolol.

## Resumo

A angiogénese ocorre quando novos vasos sanguíneos se formam a partir dos já existentes devido à proliferação de células endoteliais (ECs). Estas células que compõem o revestimento do lúmen do coração (endocárdio) e dos vasos sanguíneos e linfáticos, têm a capacidade de permanecer quiescentes por anos e rapidamente mudar para um estado de ativação em resposta a estímulos. É o equilíbrio entre fatores pró e anti-angiogénicos que determina o nível de angiogénese em curso. Quando as ECs são estimuladas por fatores pró-angiogénicos, como o VEGF-A (fator de crescimento endotelial vascular), há um aumento na proliferação, migração e diferenciação de ECs, levando à formação de um novo vaso. A angiogénese desempenha um papel importante em vários processos fisiológicos, como durante o reparo de tecidos e o ciclo reprodutivo feminino, sendo também temporariamente ativada em processos fisiopatológicos, incluindo aterosclerose, inflamação crónica e cancro.

Durante a progressão tumoral, ocorre uma proliferação rápida e descontrolada de células tumorais, levando a um microambiente hipóxico com fornecimento insuficiente de sangue contendo nutrientes e oxigénio. Como tal, as células tumorais começam a libertar fatores pró-angiogénicos. Além disso, a hipóxia leva à estabilização do HIF-1 $\alpha$  (HIF: fator induzido por hipóxia), que dimeriza com o HIF-1 $\beta$  no núcleo e atua como fator de transcrição de genes com elementos responsivos à hipóxia (HRE), tal como o VEGF. Portanto, a hipóxia tem um impacto na função das células endoteliais e na angiogénese, dado o aumento da taxa glicolítica e a proliferação de ECs devido à indução da expressão de genes envolvidos na glicólise.

Descobertas recentes sugerem que a comunicação entre as células presentes no microambiente tumoral é simbiótica, de modo a suportar a remodelação metabólica do tumor. Como tal, há partilha de moléculas orgânicas e de sinalização entre os diferentes tipos de células, cooperando para a sobrevivência do sistema. Esta relação é ainda mais importante para as células tumorais quando o acesso a nutrientes é muito baixo, contribuindo com novas fontes de energia e biomassa. Deste modo, o conhecimento das interações metabólicas poderá auxiliar na identificação de novos candidatos a alvos terapêuticos para o tratamento do cancro.

O primeiro objetivo desta tese foi investigar o efeito da hipóxia na remodelação metabólica durante a ativação das células endoteliais que poderá ocorrer no microambiente tumoral. Uma análise por espectroscopia de ressonância magnética nuclear (RMN) de HUVECs (células endoteliais da veia umbilical humana) expostas à hipóxia mimetizada por CoCl<sub>2</sub> mostrou níveis reduzidos de lactato em hipóxia, tanto intra- quanto extracelulares. No meio extracelular também foi detetado um nível inferior de 2-hidroxi-isobutirato em hipóxia em comparação à normóxia, um metabolito associado à via de degradação de valina, leucina e isoleucina. Além disso, em hipóxia foi detetado um aumento nos níveis de formato intracelular, o que pode indicar um fenótipo proliferativo devido ao envolvimento do formato na síntese de purinas. Pelo contrário, houve uma diminuição dos níveis intracelulares de glucose, lactato e acetato após exposição à hipóxia.

Em relação à ativação endotelial após hipóxia, foi realizado um ensaio de *tube forming* no qual HUVECs embutidas em matrigel são estimuladas a formar estruturas semelhantes a vasos, criando uma rede que simula o que ocorre *in vivo*. Assim, as HUVECs foram expostas a normóxia e a CoCl<sub>2</sub> para mimetizar a hipóxia, observando-se uma estimulação da formação de estruturas semelhantes a vasos por hipóxia. No entanto, foi realizado um ensaio *ex vivo*, o *rat aortic ring assay*, no qual a exposição a CoCl<sub>2</sub> resultou numa inibição da formação de ramificações de células endoteliais (*sprouting*) a partir do anel. Além disso, um ensaio de *wound healing* demonstrou inibição da migração em células expostas à

hipóxia induzida por  $\text{CoCl}_2$ . Tal faz-nos questionar se as concentrações de  $\text{CoCl}_2$  utilizadas constituem um modelo eficiente para estudo dos efeitos da hipóxia em células ECs.

A cisteína é um importante *scavenger* de *reactive oxygen species* (ROS), estando já demonstrado o seu papel na remodelação metabólica de células tumorais. Visto que as ROS atuam como moléculas pró-angiogénicas, decidimos investigar o efeito da cisteína na ativação endotelial. Um ensaio do *aortic ring* mostrou uma tendência para um aumento de *sprouting* quando exposto à cisteína, em normóxia e hipóxia, o que vai contra o esperado, visto que a eliminação dos ROS estaria associada a uma inibição da angiogénese. Para assegurar a existência de stress oxidativo, o ensaio foi também realizado na presença de  $\text{H}_2\text{O}_2$ , sendo que este induziu uma maior densidade de *branching points* comparando com o controlo. Porém estes níveis decresceram quando as células foram expostas a cisteína e  $\text{H}_2\text{O}_2$ , o que confirmou que os ROS poderão ter um papel na estimulação da angiogénese, sendo que a cisteína é capaz de reverter esse processo. Em relação à migração endotelial, num ensaio de *wound healing* observou-se que nem a cisteína nem o  $\text{H}_2\text{O}_2$  afetaram a migração das ECs. Deste modo, é necessário verificar o papel da eliminação de ROS na angiogénese, de modo a determinar se uma estratégia terapêutica anti-ROS será uma boa aposta para perturbar a angiogénese tumoral.

Muitas estratégias terapêuticas anti-angiogénicas foram desenvolvidas ao longo dos anos, mas falharam principalmente porque os mecanismos envolvidos na neoangiogénese ainda não são totalmente compreendidos. Algumas estratégias objetivam a destruição da vasculatura, afetando a sobrevivência do tumor. Contudo, ao contrário do que seria pretendido, um microambiente tumoral mais pobre em  $\text{O}_2$  (hipóxia) pode servir de estímulo à neoangiogénese. Portanto, o desenvolvimento de novas terapias anti-angiogénicas eficazes é urgente.

O propranolol é um  $\beta$ -bloqueador não seletivo, isto é, bloqueia os recetores adrenérgicos  $\beta_1$  e  $\beta_2$  com igual afinidade. Estes recetores são ativados pela epinefrina e norepinefrina, estando o seu bloqueio associado ao tratamento de hipertensão, miocardites, enxaquecas, transtornos de ansiedade e tremores. Nos últimos anos o propranolol surgiu como um tratamento para os hemangiomas pediátricos, mostrando-se eficaz na regressão destes tumores por vasoconstricção. No entanto, o seu mecanismo de ação sobre as ECs e funcionamento dos vasos permanece sob investigação. Assim, o nosso segundo objetivo foi estudar o efeito do propranolol na neoangiogénese, uma vez que os  $\beta$ -bloqueadores poderão ser uma estratégia potencialmente eficaz para perturbar a angiogénese tumoral. Foi realizado um ensaio de *tube forming* no qual o propranolol inibiu a formação de novas estruturas semelhantes a vasos e destruiu as já formadas. Os seus efeitos inibitórios estenderam-se à migração, conforme observado num ensaio de *wound healing* no qual HUVECs foram expostas a este fármaco, na presença e ausência de ROS ( $\text{H}_2\text{O}_2$ ). Uma análise de morte celular por citometria de fluxo indicou que o propranolol não afetou a viabilidade celular. Além disso, um ensaio de imunofluorescência mostrou que o propranolol afetava a expressão de alguns marcadores endoteliais (ICAM, VCAM, CD146, vWF), principalmente em tempos de exposição mais curtos. O efeito também foi avaliado *ex vivo* através de um *aortic ring sprouting assay*, no qual o propranolol inibiu a formação de estruturas a partir do anel, corroborando os resultados *in vitro*. Estes resultados sugerem que o propranolol poderá perturbar a angiogénese *in vitro*, sendo necessários mais estudos de modo a investigar o mecanismo envolvido e qual é o recetor adrenérgico,  $\beta_1$  ou  $\beta_2$ , responsável pela ativação das vias de sinalização envolvidas na inibição da angiogénese.

A remodelação metabólica envolvida durante o *sprouting* do anel aórtico também foi avaliada por espectroscopia de NMR, mostrando a expressão diferencial de metabolitos de diferentes vias metabólicas, incluindo glicólise, biossíntese de purinas, biossíntese e degradação de valina, leucina e isoleucina.

Este estudo fornece algumas ideias sobre a remodelação metabólica induzida pela hipóxia nas ECs, abrindo novas perspectivas sobre a adaptação metabólica subjacente à angiogénese que, apesar de ser um processo que envolve células não-malignas, é responsável pela progressão do cancro. Os resultados do efeito do propranolol na angiogénese reforçam a sua aplicação como alternativa terapêutica anti-angiogénica no tratamento do cancro, não apenas dos tumores vasculares, sendo um ponto de partida para novas investigações sobre os mecanismos subjacentes à sua ação.

**Palavras-chave:** Células endoteliais; Angiogénese; Microambiente tumoral; Hipóxia; Propranolol.

# Index

Agradecimientos .....	i
Abstract .....	ii
Resumo.....	iv
Index of figures .....	viii
List of abbreviations, acronyms and symbols.....	ix
1. Introduction.....	1
1.1. Cancer biology .....	1
1.2. Mechanisms of formation of new blood vessels .....	1
1.2.1. Vessel formation.....	1
1.2.2. Neo-angiogenesis.....	2
1.3. Cancer metabolism.....	3
1.3.1. Cancer cell metabolism.....	3
1.3.2. Role of tumor microenvironment (TME) in metabolic remodeling .....	4
1.3.3. Endothelial cells (ECs) metabolism.....	4
1.4. Role of hypoxia in metabolic remodeling in cancer and in neo-angiogenesis.....	5
1.5. Role of cysteine in metabolic remodeling in cancer and in neo-angiogenesis .....	5
1.6. $\beta$ -Adrenergic receptor blockade: an alternative to treat vascular tumors .....	6
2. Hypothesis and aims .....	7
3. Materials and Methods.....	7
3.1. Cell Culture .....	7
3.2. Nuclear magnetic resonance (NMR) for metabolomic detection .....	8
3.3. Tube-forming assay.....	8
3.4. Wound healing assay .....	9
3.5. Transwell migration assay .....	9
3.6. Cell death analysis by flow cytometry .....	9
3.7. Immunofluorescence.....	10
3.8. Rat aortic rings sprouting assay .....	10
3.9. Statistical analysis.....	11
4. Results.....	11
4.1. Metabolic remodeling of endothelial cells upon hypoxia.....	11
4.2. Influence of hypoxia in endothelial activation and vessel-like structures formation	13
4.3. Effect of cysteine in endothelial activation under normoxia and hypoxia.....	15
4.4. Effect of propranolol in the formation of vessel-like structures .....	17
4.5. Propranolol effect on cell viability.....	19



4.6.	Effect of propranolol on endothelial cell migration.....	19
4.7.	Effect of propranolol on transwell migration.....	21
4.8.	Impact of Propranolol in ECs markers expression.....	22
4.9.	Effect of propranolol in <i>ex vivo</i> sprouting .....	25
4.10.	Metabolic remodeling of endothelial cells – <i>ex vivo</i> model .....	25
5.	Discussion .....	27
5.1.	Main conclusions .....	29
5.2.	Future perspectives .....	30
6.	References .....	30
7.	Appendices.....	36

## Index of figures

Figure 4. 1 – NMR analysis of supernatants.....	12
Figure 4. 2 – NMR analysis of the aqueous phase.....	12
Figure 4. 3 – Effect of hypoxia on the formation of vessel-like structures and sprouting.....	14
Figure 4. 4 – Hypoxia don't affect endothelial cells migration .....	14
Figure 4. 5 – Cystine effect on aortic ring sprouting .....	15
Figure 4. 6 – Cysteine don't affect endothelial cells migration. ....	16
Figure 4. 7 – Propranolol (P) inhibits the formation of vessel-like structures by HUVECs cultured in basal medium .....	18
Figure 4. 8 – Propranolol inhibits the formation of vessel-like structures by HUVECs cultured in pro-angiogenic medium.....	19
Figure 4. 9 – Propranolol don't affect cell viability.....	19
Figure 4. 10 – Propranolol inhibits migration of endothelial cells .....	20
Figure 4. 11 – Propranolol don't affect transwell migration.....	22
Figure 4. 12 – ICAM and VCAM expression in HUVECs .....	23
Figure 4. 13 – CD146 and vWF expression in HUVECs.. ....	24
Figure 4. 14 – Propranolol inhibits aortic ring sprouting.....	25
Figure 4. 15 – Metabolites from aortic rings identified by NMR analysis .....	27
Supplementary Figure 1 – Propranolol don't affect cell viability. ....	37

## List of abbreviations, acronyms and symbols

ADRB – adrenoceptor beta	FBS – fetal bovine sérum
ANGPT – angiopoietin	FDA – Food and Drug Administration
ATCC – american type culture collection	FITC – fluorescein isothiocyanate
ATP – adenosine triphosphate	GLS – glutaminase
bFGF – basic fibroblast growth factor	GLS – glutaminase
BSA – bovine serum albumine	GLUT1 – glucose transporter
CAA – cancer associated adipocytes	GPCR – G protein-coupled receptor superfamily
CAF – cancer associated fibroblasts	GSH – reduced glutathione ´
CAM – cell adhesion molecules	GSSH – oxidized glutathione
cAMP – cyclic adenosine monophosphate	H <sub>2</sub> O <sub>2</sub> – hydrogen peroxide
CAT – cysteine aminotransferase	H <sub>2</sub> S – hydrogen sulfide
CBS – cystathionine-β-synthase	hEGF – human epidermal growth factor
CO <sub>2</sub> – carbon dioxide	HIF – hypoxia-inducible factor
CoA – Coenzyme A	HMDB – human metabolome database
CoCl <sub>2</sub> – cobalt chloride	HRE – hypoxia-responsive element
CSE – cystathionine-γ-lyase	HUVECs – human umbilical vein endothelial cells
CTCF – corrected total cell fluorescence	ICAM – intercellular adhesion molecule (CD54)
CTL – control	IGF – insulin growth factor
Cys – cysteine	IH – infantile hemangioma
D <sub>2</sub> O – deuterated water	LDHA – lactate dehydrogenase
DAPI – 4'-6-diamidino-2-phenylindole	LSGS – low serum growth supplement
Dll4 – delta-like ligand 4	MAPK – mitogen activated protein kinase
DNA – deoxyribonucleic acid	min – minutes
EBM – endothelial cell growth basal medium	MMPs – matrix metalloproteinases
EC – endothelial cell	MpST – 3-mercapto-pyruvate sulphurtransferase
EDTA – ethylenediaminetetraacetic acid	mRNA – messenger ribonucleic acid
EPC – endothelial progenitor cell	
ERK – extracellular signal–regulated kinases	
FAs – fatty acids	

NADPH – nicotinamide adenine dinucleotide phosphate

NF- $\kappa$ B – nuclear factor kappa B

NMR – nuclear magnetic resonance

NO – nitric oxide

ODD – oxygen-dependent domain

OXPPOS – oxidative phosphorylation

P or Prop – propranolol

PBS – phosphate buffered saline

PDK1 – pyruvate dehydrogenase kinase 1

PFKFB3 – 6-Phosphofructo-2-Kinase/Fructose -2,6-Biphosphatase 3

PHD – prolyl hydroxylase

PI – propidium iodide

PI3K – phosphatidylinositol-4,5-bisphosphate 3-kinase

PKA – protein kinase A

PlGF – placenta derived growth factor

PPP – pentose phosphate pathway

PS – phosphatidylserine

RNA – ribonucleic acid

ROS – reactive oxygen species

RQ-PCR – Relative quantifying polymerase chain reaction

TAM – tumor associated macrophages

TCA – tricarboxylic acid cycle or Krebs cycle

TEC – tumor-associated endothelial cell

TME – tumor microenvironment

TNF $\alpha$  – tumor necrosis factor alpha

VCAM – vascular cell adhesion molecule (CD106)

VEGF – vascular endothelial growth factor

VEGFRs – vascular endothelial growth factor receptor

VHL – von Hippel-Lindau

vWF – von Willebrand factor

WHO – World Health Organization

# 1. Introduction

## 1.1. Cancer biology

According to the World Health Organization (WHO), cancer is the second leading cause of death globally and is estimated to account for 9.6 million deaths in 2018,<sup>1</sup> being considered a major public health problem. Cancer occurs when there is a malfunction of the mechanisms that maintain normal cell proliferation, causing uncontrollable cell division, in a process termed carcinogenesis.<sup>2</sup> Such impairment in cellular regulation can result from genetic damage that can be caused by tumor-promoting chemicals, ionizing radiations, hormones, viruses or even replication errors and spontaneous chemical reactions.<sup>3</sup> Overall, carcinogenesis has its onset in mutations of three classes of genes: mutations of **proto-oncogenes** that turn them into **oncogenes** that promote tumor growth; mutations that inactivate **tumor-suppressor genes**, allowing abnormal cell division and survival.<sup>2,4</sup> Besides genetics, epigenetic modifications can contribute for carcinogenesis by alterations in DNA methylation and in the activity of enzymes that modify histones, and consequently chromatin remodeling.<sup>3,5</sup>

A tumor is considered malignant when its cells exhibit cell dysplasia (abnormal morphology) and in advanced stages are capable of invading and spreading to form metastases (secondary tumors).<sup>6</sup> Tumor progression also depends on the non-neoplastic cells (such as stromal and endothelial cells) present in the tumor microenvironment (TME), acting as a network that shares signaling and organic molecules.<sup>7</sup>

In 2000, Hanahan and Weinberg proposed six biological capabilities and cellular traits that are acquired during the development of tumors: sustaining proliferative signaling; evading growth suppressors; resisting cell death; enabling replicative immortality; inducing angiogenesis; activating invasion and metastasis.<sup>8</sup> In 2011 they and others revisited these hallmarks and considered new features: genome instability and mutation and tumor-promoting inflammation (considered enabling characteristics) and reprogramming energy metabolism and evading immune destruction (two emerging hallmarks).<sup>7,9</sup> Altogether, the hallmarks were helpful to better understand carcinogenesis, even though there is still a lot to learn.

## 1.2. Mechanisms of formation of new blood vessels

### 1.2.1. Vessel formation

Blood vessels are responsible for the supply of nutrients and oxygen to all tissues in the body, in addition to provide immune surveillance. There are several mechanisms that drive the formation of blood vessels. During embryogenesis, the assembly of new endothelial cells into a primitive vascular plexus is called **vasculogenesis**.<sup>10,11</sup> Additionally, **neovascuogenesis** occurs in adult when endothelial progenitor cells (EPCs) are mobilized from the bone marrow to differentiate into endothelial cells (ECs) and start the *de novo* formation of a vessel.<sup>10,12</sup> **Vascular mimicry** is a phenomenon resembling a vessel formation process that is responsible for increased cancer resistance to some therapies. This mechanism consists in cancer cells starting to behave as ECs, even co-expressing some ECs markers and being able to form structures similar to vessels.<sup>10</sup> Nevertheless, when new blood vessels sprout from pre-existing blood vessels through proliferation of ECs the process is called **angiogenesis**. Angiogenesis is transiently activated in several physiological processes, such as tissue repair and in the female reproductive cycling, and in various pathologies including cancer, atherosclerosis, and chronic inflammation.<sup>13</sup>

Angiogenesis is regulated by pro- and anti-angiogenic factors that either induce or inhibit the sprouting. Among the positive regulators, VEGF-A (vascular endothelial growth factor-A commonly designed solely VEGF) is the most well-studied and it is observed almost ubiquitously at angiogenesis sites.<sup>14</sup> This growth factor is released by tumor cells and once it binds to its tyrosine kinases receptors (VEGFRs) they become activated and dimerize (homo or hetero), triggering an intracellular signaling cascade. For example, Ras, Src, and PI3K (phosphatidylinositol kinase) /Akt pathways are activated by VEGFR2.<sup>15</sup> The VEGF signaling pathway is involved in several steps of angiogenesis, such as ECs proliferation, migration, differentiation, tube formation and permeability control, either in physiological and pathophysiological conditions.<sup>16</sup>

Angiogenesis is a multi-step process. First, vasodilation and an increase of vascular permeability occur at the same time of pericytes (supportive mural cells) detachment and then the basement membrane that surrounds the capillaries is degraded. This allows the activation of ECs, which will proliferate and initiate the formation of the new tube, followed by the formation of the new extracellular matrix.<sup>10</sup>

ECs constitute the inner lining of blood and lymphatic vessels. In healthy adults, these cells have the capacity to remain quiescent for years but rapidly switch to a highly plastic state in response to stimuli such as hypoxia (reduced oxygen availability) or growth factors.<sup>17,18</sup> There are three subtypes of endothelial cells. After a pro-angiogenic stimuli gradient (e.g. VEGF – vascular endothelial growth factor), the **migratory tip cells** become motile (with numerous filopodia) and guide the growing sprout, being followed by the **stalk cells** that proliferate and elongate. Lining the newly established vessel are the **quiescent phalanx cells**, that regulate vascular homeostasis and the barrier function. Mural cells, as pericytes, are recruited to stabilize the new connections. These cells share a basement membrane with ECs, that needs to be degraded at the beginning of sprouting by matrix metalloproteinases (MMPs).<sup>19</sup>

Interestingly, the phenotype of ECs is not genetically predetermined, it is dynamically selected in response to cell competition for growth factors, allowing the fittest cell to acquire the tip position. The key regulator for this lateral inhibition is VEGF, hence the cells closest to the site with the highest VEGF level will be selected as tip cells.<sup>18</sup> Upon reaching the tip cell, VEGF binds to its receptor VEGFR2, which induces delta-like ligand 4 (Dll4) expression. The neighbor EC binds its Notch receptor to Dll4, stimulating the expression of VEGF receptor 1 (VEGFR1) while decreasing VEGFR2 expression. Ultimately this leads to the increase of VEGFR1/VEGFR2 ratio which lowers the EC responsiveness to VEGF, since VEGFR1 has lower affinity to VEGF than VEGFR2, acting as a VEGF trap. Consequently, a stalk phenotype is imposed in the latter EC, turning the first in the tip cell, which will be able to contact with another tip cell and coalesce, forming the new sprout towards the gradient of the growth factor.<sup>11,17</sup>

### 1.2.2. Neo-angiogenesis

During tumor progression an “angiogenic switch” is activated, excessively stimulating proliferation and migration of ECs to form new vessels, giving tumor cells better access to nutrients and oxygen. As a matter of fact, the relationship between neo-vessels and tumor growth was first proposed by Judah Folkman.<sup>20</sup> He also suggested a relationship between neo-angiogenesis and the malignancy of a tumor,<sup>21</sup> since these neo-vessels can be used as routes for neoplastic cells to metastasize.

Anti-angiogenic strategies consist in the treatment with an angiogenesis inhibitor (e.g. VEGF signaling blockade) to stimulate the regression of the vessels and the starvation of tumor cells, leading

to tumor regression.<sup>17</sup> So far, these strategies have failed, in part because the precise molecular and biologic mechanism during cancer neo-angiogenesis still remains unclear.

The blood vessels formed within tumors are structurally and functionally abnormal. This aberrant vasculature is characterized by excessive vessel branching, leakiness, enlarged, distorted and tortuous vessels and even mural cells are less abundant.<sup>22</sup> These weak ECs junctions will facilitate intravasation of cancer cells due to its increased leakiness. Moreover, by destroying the vascular supply, anti-angiogenic strategies increase hypoxia within the TME. Consequently, cancer cells adapt and acquire a non-oxidative metabolism, depending less on oxygen and increasing its resistance to anti-angiogenic treatment.<sup>23</sup> Due to this dysfunctionality, the efficacy of chemotherapy drug delivery is reduced. Therefore, new findings in tumor vessel normalization (by targeting ECs metabolism) could improve drug delivery,<sup>24</sup> once it partially restores the normal structure of tumor vessels, by improving perfusion and tightening the vascular barrier (decreasing leakiness). In combination with chemotherapy this could efficiently impair metastasis.<sup>22</sup>

### 1.3. Cancer metabolism

#### 1.3.1. Cancer cell metabolism

Cancer cells have characteristic metabolic alterations necessary for the acquisition of nutrients in a nutrient-deficient environment, essential for the production of biomass that will sustain the high proliferative rate.<sup>25</sup> For instance, cancer cells exhibit high glucose uptake and increased rates of glycolysis and lactate production (Warburg Effect), even in the presence of oxygen.<sup>23,26</sup> This process is usually termed “aerobic glycolysis” and accounts for high lactate concentrations in the TME, which becomes more pro-angiogenic. Currently, it is known that aerobic glycolysis is independent of the oxidative phosphorylation (OXPHOS) accomplishment.<sup>27</sup> Contrarily to Otto Warburg’s hypothesis that tumor mitochondria have impaired cellular respiration, in most type of tumors OXPHOS remains functional.<sup>28</sup> For example, AS-30D tumor cells (hepatoma cells) have a predominantly oxidative type of metabolism, being extremely sensitive to OXPHOS inhibitors.<sup>29,30</sup>

Glutamine substitutes glucose in all metabolic intercourses.<sup>31</sup> Glutamine can be converted into glutamate, by the enzymatic action of glutaminase (GLS),<sup>32</sup> entering the TCA cycle (tricarboxylic acid cycle or Krebs cycle) as  $\alpha$ -ketoglutarate, leading to NADPH regeneration and the production of citrate, which can be used for the production of acetyl-groups (such as acetyl-CoA) and for fatty acids (FAs) synthesis.<sup>25,33</sup>

Cysteine (Cys) is a semi-essential amino acid synthesized primarily in the liver and required for general protein biosynthesis. Cystine, the oxidized form of Cys, is transported into cell by the  $x_c^-$  antiporter system, in exchange for glutamate.<sup>34,35</sup> Cystine is rapidly converted to Cys in the intracellular milieu, being able to enter in the glutathione (GSH) biosynthetic pathway.<sup>34</sup> GSH is a tripeptide composed of glutamate, Cys, and glycine that avoids cellular oxidative stress by acting as a free radical scavenger and detoxifying agent.<sup>36</sup> Increased metabolic activity, mitochondrial dysfunction and peroxisome activity are the major sources of reactive oxygen species (ROS) in cancer cells,<sup>37</sup> so there is a high demand of Cys for GSH synthesis.<sup>38</sup>

Since cancer cells are highly proliferative, there is a need for membrane molecules biosynthesis. Membrane lipids, such as phospholipids, contain FAs, the “cellular building blocks”.<sup>33</sup> In tumors the *de novo* synthesis of FAs takes place in simultaneous with degradation ( $\beta$ -oxidation)<sup>39</sup>. FAs are also

required for energy storage and synthesis of signaling molecules, as well as a source of acetyl-CoA, through  $\beta$ -oxidation, to supply OXPHOS.<sup>40</sup>

### **1.3.2. Role of tumor microenvironment (TME) in metabolic remodeling**

Apart from the neoplastic cells, in the TME there are endothelial cells, cancer associated fibroblasts (CAFs), cancer associated adipocytes (CAA), tumor associated macrophages (TAMs) and other immune cells (e.g. B and T cells).<sup>41</sup>

Recent findings suggest that the communication between the cells in the TME is symbiotic to support tumor metabolism, maintenance, and growth. Therefore in the TME, there are shared organic and signaling molecules, produced from different cell types, cooperating and allowing the entire system's survival.<sup>41–43</sup> This sharing is even more important to cancer cells when the nutrients levels are very low, filling their demands with new sources of energy and biomass. The knowledge about these metabolic interactions has the potential to update the list of new cancer therapies candidates.<sup>6,44</sup>

### **1.3.3. Endothelial cells (ECs) metabolism**

Normal ECs (i.e., under non-pathological circumstances) rewire their metabolism to meet the high demands (energetic and biosynthetic) of the physiological state. ECs resemble cancer cells in their preference to use glycolysis rather than OXPHOS when it comes to glucose metabolism.<sup>11,22,45</sup> Although it seems counterintuitive given the lower ATP production comparing to mitochondrial respiration, this will sustain lactate production, which will stimulate angiogenesis.<sup>18</sup> Moreover, by abstaining from the use of oxygen, ROS are kept in a minimum and high oxygen concentrations are maintained in the blood to distribute for the perfused tissues. By using this oxygen-independent pathway, ECs are able to migrate through hypoxic environments without major adaptations to their metabolism. This also sustains macromolecule synthesis by feeding glycolytic side branches with carbons from glucose. In the case of the pentose phosphate pathway (PPP), ribose-5-phosphate is produced and used for the synthesis of nucleic acids. This pathway also regulates redox homeostasis, influencing cell viability and angiogenesis. This occurs due to the formation of NADPH, which is used in the conversion of oxidized glutathione (GSSG) to reduced glutathione (GSH) by GSH reductase. NADPH is also required for the synthesis of lipids and nitric oxide (NO).<sup>11</sup>

However, if glucose levels decrease significantly, anaerobic glycolysis is impaired (Crabtree effect)<sup>46</sup> and ECs can switch to OXPHOS metabolism since mitochondria remain functional.<sup>47</sup> In addition, ECs store glucose as glycogen reserves, probably to have an endogenous source of glucose as a backup for energy under glucose-deprived conditions.<sup>22,23</sup>

A compartmentalization of glycolytic enzymes (e.g. 6-Phosphofructo-2-Kinase/Fructose-2,6-Biphosphatase 3 (PFKFB3)) occurs in the filopodia and lamellipodia, the migratory structures of ECs, where mitochondria are excluded. This localization is due to an association with F-actin, allowing a rapid ATP production (“ATP hot spots”) to fuel actin-myosin contraction and a cytoskeleton remodeling during cell migration.<sup>11,45</sup>

Similar to cancer cells, glutamate is also the most abundant intracellular amino acid in endothelial cells.<sup>11</sup> Glutamine contributes to TCA cycle anaplerosis, arginine metabolism and also nucleotide synthesis. In addition, OXPHOS is still functioning, producing reducing equivalents to sustain ATP production.

Comparative to ECs in physiological circumstances, **tumor-associated ECs (TECs)** have a further increased glycolytic flux, evidenced by an increased expression of GLUT1 (glucose transporter) and PFKFB3<sup>17</sup>. These cells are hyperproliferative, demanding more substrates for energy production and more metabolites for biomass synthesis, being this the reason why they also retain functional mitochondria. In fact, TECs are more angiogenic, more responsive to pro-angiogenic signaling, and often more resistant to chemotherapeutic and anti-angiogenic drugs. The secretome of cancer cells induces responses in TECs, for example cancer cells can stimulate the glucose uptake by TECs and cancer cells secrete lactate, which induces EC proliferation.<sup>22</sup>

#### **1.4. Role of hypoxia in metabolic remodeling in cancer and in neo-angiogenesis**

Hypoxia is a characteristic feature of several pathological conditions, including cancer and cardiovascular disease.<sup>48</sup> The TME becomes hypoxic due to the insufficient blood supply when rapid tumor growth occurs.

The hypoxia response occurs through the activation of hypoxia-inducible factors (HIFs), a family of transcription factors composed by an oxygen-sensitive subunit (HIF-1 $\alpha$ ) and a constitutively expressed subunit (HIF-1 $\beta$ ).<sup>49</sup> In normoxia, oxygen binds to oxygen-dependent enzymes, the prolyl hydroxylases (PHDs), which hydroxylate two proline residues of HIF-1 $\alpha$  on the oxygen-dependent domain (ODD).<sup>50</sup> This reaction inhibits the dimerization with the HIF-1 $\beta$  subunit, since it promotes binding to von Hippel-Lindau tumor suppressor (pVHL), which is part of an E3 ubiquitin ligase complex, targeting HIF-1 $\alpha$  with ubiquitin for consequent proteasomal degradation.<sup>49,51</sup> In contrast, in hypoxic conditions the PHDs don't promote HIF-1 $\alpha$  hydroxylation, since the oxygen is missing. Thus HIF-1 $\alpha$  accumulates, translocate to the nucleus, where dimerizes with HIF-1 $\beta$  forming the heterodimer, being the dimerization required for DNA binding. The dimer acts as a functional transcription factor, leading to the activation of target genes with specific DNA sequences, named hypoxia-responsive elements (HRE).<sup>17,52</sup> VEGF expression is induced by hypoxia, since the corresponding gene has an HRE region, which will induce ECs proliferation and subsequently neo-angiogenesis.<sup>12</sup>

Hypoxia has an impact in ECs function and angiogenesis, hence HIF-1 $\alpha$  stabilization induces activation of pro-angiogenic genes (VEGF, angiopoietin 1 (ANGPT1), placenta derived growth factor (PlGF)), increases the expression of genes involved in glycolysis (e.g. GLUT1, PFKFB3) resulting in a higher glycolytic rate and increased ECs proliferation<sup>17</sup>. Hypoxia leads to higher glycolysis rates by upregulation of glycolysis-promoting genes, such as GLUT1, PFKFB3, Lactate dehydrogenase (LDHA), Pyruvate dehydrogenase kinase 1 (PDK1). Metabolic pathway analysis of ECs exposed to hypoxia indicated increased amino acids biosynthesis, carbon metabolism, promotion of the PPP and Cys/methionine metabolism.<sup>17</sup>

#### **1.5. Role of cysteine in metabolic remodeling in cancer and in neo-angiogenesis**

Recently our team published several papers showing the relevance of thiols (cysteine included) in cancer metabolism and therapy escape.<sup>53,54</sup> As one of the components of GSH, an important ROS scavenger, Cys plays an important role in the maintenance of the redox equilibrium. At non-toxic levels, ROS act as pro-angiogenic molecules, being important modulators of endothelial cells. All things considered, Cys can be relevant in endothelial activation or, at least, as a ROS scavenger.



Hydrogen sulfide (H<sub>2</sub>S) is synthesized in ECs by three enzymes that degrade Cys: cystathionine- $\gamma$ -lyase (CSE), cystathionine- $\beta$ -synthase (CBS) and by 3-mercapto-pyruvate sulphurtransferase (MpST) accompanied by cysteine aminotransferase (CAT). The production of H<sub>2</sub>S in ECs stimulates angiogenesis by promoting ECs repair, proliferation and migration, inhibiting vascular inflammation and increasing production of GSH, which decreases oxidative stress.<sup>11,55</sup>

However, the role of H<sub>2</sub>S on cancer is still controversial, once tumors exposed to H<sub>2</sub>S exhibit two opposite behaviors, a pro-cancer and an anti-cancer effect. There are many mechanisms that contribute to the pro-cancer effect: induction of angiogenesis; regulation of mitochondrial bioenergetics; acceleration of cell cycle progression, and anti-apoptosis function.<sup>55,56</sup> Contrarily, H<sub>2</sub>S can also inhibit the cancer cell proliferation through induction of cell cycle arrest, promotion of apoptosis and induction of cell injury due to uncontrolled intracellular acidification.<sup>55</sup> Therefore, there may be a balance between the effects induced by H<sub>2</sub>S, which depends on each particular cancer cell context.

### **1.6. $\beta$ -Adrenergic receptor blockade: an alternative to treat vascular tumors**

Adrenoceptor beta 2 (ADRB2) is the gene that encodes the  $\beta_2$ -adrenergic receptor. This cell surface receptor is a member of the G protein-coupled receptor superfamily (GPCRs).<sup>57</sup> The activation of these receptors by epinephrine or norepinephrine,<sup>58</sup> leads to the stimulation of adenylate cyclase, that results in increased cAMP (cyclic adenosine monophosphate) levels and activation of protein kinase A (PKA).<sup>59</sup> This may also result in the activation of mitogen activated protein kinase (MAPK) pathway, phosphatidylinositol-4,5-bisphosphate 3-kinase (PI3K) and Akt/protein kinase B.<sup>60</sup>

Propranolol is a non-selective  $\beta$ -blocker (which competitively blocks  $\beta_1$  and  $\beta_2$ -adrenoceptors with equal affinity)<sup>61</sup> usually used for the management of hypertension, myocardial infarction, migraines, anxiety disorders and tremor.<sup>62</sup> In the last years, this antagonist has emerged as an effective treatment to infantile hemangiomas (IH), since it promotes the regression of these tumors by vasoconstriction,<sup>63</sup> being already FDA approved to IH. These are the most common benign tumors of infancy and involve accumulation, proliferation, and differentiation of aberrant vascular structures.<sup>63,64</sup> However, its specific mechanism(s) of action remain unknown, although there is some knowledge of how propranolol interferes with endothelial cells and, thereby, angiogenesis. For example, propranolol induces a downregulation of proangiogenic proteins (such as VEGF, bFGF, MMPs) and inhibits the ERK/MAPK signaling pathway, thus inhibiting angiogenesis.<sup>64,65</sup> The elucidation of the mechanism underlying vessels disruption by propranolol, will be a major challenge for the near future, since it can have a potential to target angiogenesis and treat cancer.

## 2. Hypothesis and aims

Our first hypothesis is that endothelial cells undergo a metabolic remodeling to sustain cancer angiogenesis, being this process controlled by microenvironment. Therefore, the first objective of this thesis is to disclose the influence of hypoxia (an important microenvironmental component) in the metabolic remodeling during the endothelial cell activation.

Our second hypothesis is that  $\beta$ -blockers, such as propranolol, can be a potential cancer therapy by disrupting tumor angiogenesis. Accordingly, our second objective is to determine the effect of propranolol on *bona fide* vascularization.

## 3. Materials and Methods

### 3.1. Cell Culture

Human umbilical vein endothelial cells (HUVECs: CRL-1730, ATCC) were used as *in vitro* model of human endothelium for the study of tumor-associated angiogenesis. These cells were cultured in Endothelial Cell Growth Basal Medium-2 (EBM-2: CC-3156, Lonza, Bioscience) supplemented with EGM-2 SingleQuots Supplements (CC-4176, Lonza, Bioscience): 2% FBS, hydrocortisone, hFGF-B, VEGF, R3-IGF-1, ascorbic acid, hEGF, GA-1000 and heparin. The cell culture was maintained at 37°C in a humidified environment of 5% CO<sub>2</sub>. Cells were plated on gelatin-coated T75 flasks (75 cm<sup>2</sup>) and cultured to 75 - 100% optical confluency before they were detached with 0.05% trypsin-EDTA 1X (25300-054, Invitrogen) at 37°C for 2 - 3 min. For each assay a Bürker counting chamber was used to determine the cell number necessary.

Cells were exposed to CoCl<sub>2</sub> (100  $\mu$ M; C-8661, Sigma-Aldrich), L-cysteine (Cys; 402  $\mu$ M; 102839, Merck), propranolol (100  $\mu$ M; P8688, Sigma) and H<sub>2</sub>O<sub>2</sub> (15  $\mu$ M).

For the NMR assay (3.2), HUVECs were plated in 90 mm cell culture dishes (55 cm<sup>2</sup>) (2 x 10<sup>5</sup> cells/mL) and maintained in EBM-2 all in. The experimental conditions were added on the next day (6h incubation).

For tube forming assay (3.3), cells (1.5 × 10<sup>5</sup> cells/mL) were plated in 48-well plates and exposed to the experimental conditions for 6 h.

For wound healing assay (3.4), cells (2 × 10<sup>5</sup> cells/mL) were plated in 24-well plates and cultured until reaching a confluent monolayer. After incubation with mitomycin-C to inhibit proliferation, the scratch (wound) was made, cells in suspension were removed and adherent cells were exposed to the experimental conditions for 24 h.

For the migration transwell assay (3.5), cells (5 × 10<sup>5</sup> cells/mL) were plated in the 12  $\mu$ m 8  $\mu$ m-pore inserts. Cells were then exposed to the experimental conditions for 6 h.

In cell death analysis (3.6), cells (2 × 10<sup>5</sup> cells/mL) were plated in 24-well plates. After starvation (FBS-free culture medium) overnight, cells were exposed to the experimental conditions for 6h.

For the immunofluorescence technique (3.7), cells (1.6 × 10<sup>5</sup> cells/mL) were plated in  $\mu$ -slide 8 well. After reaching confluency the experimental conditions were added (6h incubation).

### 3.2. Nuclear magnetic resonance (NMR) for metabolomic detection

NMR is one of the main techniques used in metabolomics analysis, given the easy sample preparation, the ability to quantify the most abundant compounds and its high reproducibility.<sup>66</sup> This technique is mostly used for untargeted analysis and when allied with isotopically enriched <sup>13</sup>C molecules allows the tracking of the metabolic pathways that incorporated this isotope.<sup>67</sup>

Therefore, NMR assay was performed to identify the effect of hypoxia on endothelial cell metabolism. HUVECs were plated in 90 mm cell culture dishes (55 cm<sup>2</sup>) (2 x 10<sup>5</sup> cells/mL) and maintained in EBM-2 all in. On the next day, cells were treated with 10 mM lactate (20% <sup>13</sup>C-lactate (sodium <sup>13</sup>C-L-lactate; CX1585V; Sigma) + 80% lactate (Sodium lactate; 106522.2500; Merck)), 5 mM glucose (G8270, Sigma) and 5 mM glucose (9% <sup>13</sup>C-glucose (389374; Sigma-Aldrich) + 91% <sup>12</sup>C-glucose), in the presence and absence of hypoxia (mimicked by 100 μM CoCl<sub>2</sub>) in Complete Endothelial Cell Medium supplemented with VEGF, EGF, L-Glutamine, antibiotic-antimycotic solution and FBS from the kit (1168, Cell Biologics). After 6h incubation, the supernatants were collected and stored at -20°C. Cells were harvested with PBS 1X (washed twice), scraped and centrifuged at 155 g for 10 min. Methanol and chloroform extraction was performed to separate organic and aqueous phases. Cold methanol was added to the cell pellets (4ml methanol/1g cell pellet), followed by water (twice the volume of methanol). After a 5 min incubation on ice, chloroform (the same volume of methanol) was added to the mixture, followed by water (the same volume of methanol). The samples incubated 10 min on ice and were centrifugated at 1700 g for 15 min at 4°C. Both organic and aqueous phases were collected with a glass pipette and stored at -20°C. The remaining sample preparation was performed at ITQB Oeiras. A phosphate buffer with deuterated water (D<sub>2</sub>O) was added to the aqueous phases. Both <sup>1</sup>H and <sup>13</sup>C spectra were acquired in a magnetic field of 500 MHz in Ultrashield™ 500 Plus (Bruker).

Aortic rings were also analyzed by NMR. After the sprouting assay, the rings were extracted from matrigel, washed with PBS 1X and stored at -80°C. Then we added cold methanol, followed by homogenization with a tissue homogenizer. The rest of the extraction was done accordingly to the methanol and chloroform extraction mentioned previously. The spectra acquisition was made in a magnetic field of 800 MHz in Ultrashield™ 800 Plus (Bruker) at ITQB Oeiras.

All the spectra analysis was done according to Chenomx NMR suite 8.1 and Human Metabolome database (HMDB) in TopSpin 3.2 software.

### 3.3. Tube-forming assay

Tube-forming assay is an *in vitro* experiment that focuses on the angiogenesis stage whereby endothelial cells form the vessel sprout, differentiating into vessel-like structures, forming a network that simulates what occurs *in vivo*.<sup>68,69</sup> This assay relies on the presuppose that ECs are induced to form tube-like structures when cultured on a matrix of basement membrane extract.

One day prior to assay, the cell medium was replaced by 200 PRF medium (M-200-500, Gibco) supplemented with LSGS (S-003-10, Gibco). A 48-well plate was coated with matrigel (354230, Corning) and incubated at 37°C for 30 min to solidify. HUVECs were incubated with calcein (C1430, Invitrogen), a fluorescent cell permeable dye, for 30 min at 37°C and 5% CO<sub>2</sub>.

Cells were harvested and resuspended in a basal medium (200 PRF supplemented with FBS; S0615, Thermo Fisher Scientific) or in a pro-angiogenic medium (200 PRF supplemented with LSGS, FBS and bFGF) where the experimental conditions were added. Representative images of the tube-like

structures formation were acquired at 4 h and 6 h in an Olympus IX53 Inverted Microscope and analyzed with ImageJ software ([imagej.nih.gov/ij/](http://imagej.nih.gov/ij/)).

### 3.4. Wound healing assay

Wound healing assay is a method to measure the directional 2D cell migration *in vitro*, used to investigate the effect of compounds or genetic manipulation on cell migration.<sup>13,70</sup> This assay was performed to determine the effect of hypoxia (mimicked by CoCl<sub>2</sub>), ROS (H<sub>2</sub>O<sub>2</sub>) and propranolol ( $\beta$ -blocker) on ECs cell migration. Cells were plated on gelatin-coated 24-well plates and allowed to form a confluent monolayer. Once confluent, cells were incubated for 3 h with mitomycin-C (M4287, Sigma), an antimitotic agent that inhibits cell proliferation. A linear scratch in each monolayer was made with a P200 pipette tip, creating a gap across the well diameter. The media was replaced to remove debris and cells in suspension and to expose cells to the experimental conditions. Bright-field images of each well were acquired on the Olympus IX53 Inverted Microscope at the following timepoints: 0, 2, 4, 6 and 24h (0, 2, 4, 6, 8, 10 and 24h for experiments with propranolol). Images were analyzed and quantified by ImageJ software.

### 3.5. Transwell migration assay

Transwells assays (or Boyden chamber assays) are a useful tool to study cell migration and invasion.<sup>71</sup> To determine the effect of hypoxia and propranolol on migration of ECs *in vitro*, transwell inserts with 8- $\mu$ m pore size polycarbonate membrane (PI8P01250, Millicell) were used. Cells were incubated in FBS free media overnight and the underside of the insert membrane was coated overnight at 4°C with EBM-2 containing 10  $\mu$ g/ml gelatin (G-1890, Sigma Aldrich).

Cells were harvested and resuspended in EBM-2 without FBS, while the lower chamber was loaded with EBM-2 with FBS and the experimental conditions. Cells incubated at 37°C in a humidified environment of 5% CO<sub>2</sub> for 6 h. At the end the upper filter membrane was wiped with a cotton swab to remove cells that didn't migrate through the filter to the lower chamber. After washing with PBS 1X, cells in the lower surface of the filter were stained with 0.5% (w/v) crystal violet in 25% methanol for 10 min at room temperature. After washing with 10% methanol, representative images were acquired with the Olympus SZX12 Stereozoom Microscope and Olympus IX53 Inverted Microscope. The number of cells that migrated through the transwell membrane was assessed using ImageJ software.

### 3.6. Cell death analysis by flow cytometry

The cell viability analysis was made by FITC labeled-annexin V/propidium iodide (PI) staining. When cells undergo apoptosis the phosphatidylserine (PS) present on the inner surface of the membrane translocate to the cell surface. This exposition allows the binding of the labeled annexin V (640906, BioLegend) in a calcium-dependent manner.<sup>72</sup> To differentiate between early apoptotic cells from membrane permeabilized cells (late apoptotic and necrotic cells), we use PI (P4170, SigmaAldrich) that is a fluorogenic compound that only binds to double stranded DNA. PI is not permeant to live cells, thus staining only membrane permeabilized cells.<sup>73</sup> By flow cytometry the percentage of viable, early apoptotic, late apoptotic and necrotic cells is assessed.

In the context of the present thesis, this assay was performed to analyze the effect of propranolol in HUVECs viability. Plated cells were incubated overnight with EBM-2 media without serum (FBS). After experimental conditions (6 h incubation), supernatants were collected, cells were harvested with trypsin and centrifuged at 155 g for 5 min. Cell pellets incubated with FITC labeled-annexin V in annexin V binding buffer 1X at room temperature for 15 min in dark. After incubation, cells were resuspended in PBS 1X 0.1% (v/w) BSA and centrifuged at 155 g for 2 min. The remaining pellet was resuspended in annexin V binding buffer 1X and PI and analyzed by flow cytometry. FlowJo X v10.0.7 software was used to analyze the data obtained.

### 3.7. Immunofluorescence

Immunofluorescence is a microscope-based technique used to detect specific target antigens by using antibodies labelled with fluorochromes. In this thesis indirect immunofluorescence was performed, in which a primary unlabeled antibody binds to the target and then this is recognized by the secondary antibody that is fluorophore-labeled.<sup>74</sup>

Cells were plated in  $\mu$ -slide 8 well (80826, ibidi), previously coated with poly-lysine (L7240, Biochrom). After 6 h incubation with the experimental conditions, cells were fixed in 2% (w/v) paraformaldehyde (104003, Merck Millipore) for 15 min at 4°C, blocked with 0.1% PBS-BSA / 0.1% Triton X-100 for 30 min at room temperature and incubated overnight with primary antibody (diluted in 0.1% (w/v) PBS-BSA). The antibodies used were from Endothelial cell characterization kit (SRC023, Millipore; anti-ICAM (1:500), anti-VCAM (1:500), anti-CD146 (1:500), anti-vWF (Abcam, 1:5000).

After washing with PBS 1X, cells were incubated with the secondary antibodies for 2 h, at room temperature. The secondary antibodies (diluted in 0.1% (w/v) PBS-BSA, 1:1000) used were: Alexa Fluor 488 goat anti-mouse (115-545-003, Thermo fisher scientific), Alexa Fluor 594 donkey anti-mouse (A21203, Thermo fisher scientific) and Alexa Fluor 594 goat anti-rabbit (ab150080, Abcam). In this technique a negative control is necessary to confirm the specificity of the secondary antibody, being stained without primary antibodies. After washing with PBS, all samples were stained with VECTASHIELD media with DAPI (4'-6-diamidino-2-phenylindole; Vector Labs), which stains the nucleus. Images were acquired in an Olympus IX53 Inverted Microscope and analyzed with ImageJ software.

### 3.8. Rat aortic rings sprouting assay

The rat aortic ring sprouting assay is an *ex vivo* assay that consists in the grow of angiogenic vessels from a segment of a rat aorta (ring).<sup>75</sup> This is a useful procedure to study the sprouting angiogenesis, being more functionally relevant than other *in vitro* assays.<sup>76,77</sup>

Aortas (thoracic and abdominal segments) were dissected from rats and then cleaned to remove external tissue and flush off blood from the lumen. After removing all extraneous fat and fibrotic tissue and branching vessels, the aorta was segmented into rings with approximately 1 mm. The rings were transferred to a Petri dish and incubated overnight in FBS-free culture medium at 37°C, 5% CO<sub>2</sub>. The next day rings were embedded in matrigel (supplemented with the experimental conditions) in a 24-well plate and fed with EBM-2 supplemented with the experimental conditions. The medium was replaced every 3-4 days and the sprout is visible at 7-10 days. Representative images were acquired at day 10 on the Olympus IX53 Inverted Microscope and were analyzed by ImageJ software. The sprouting

quantification was performed by counting the number of branch points per sprouting area (area around and inside the ring were sprouting was visible), which is the cell network density, that was then normalized to the respective control, obtaining the branch points density.

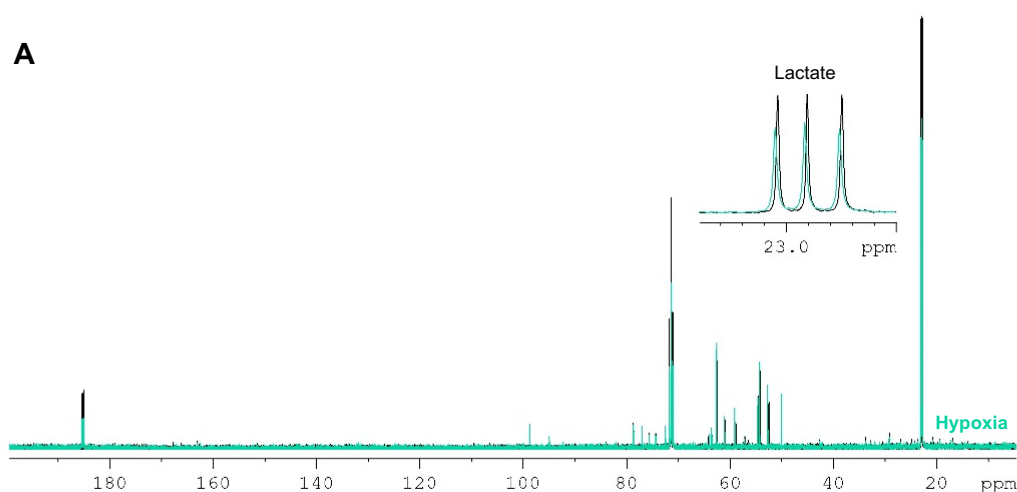
### 3.9. Statistical analysis

All results were analyzed by GraphPad Prism 7.00 software ([www.graphpad.com/](http://www.graphpad.com/)), using student's t test, one-way ANOVA or two-way ANOVA to evaluate the statistical significance of results. The assays were performed with, at least, 3 replicates per condition and the differences were considered statistically significant at  $p < 0.05$ .

## 4. Results

### 4.1. Metabolic remodeling of endothelial cells upon hypoxia

To understand the effect of hypoxia on endothelial cells metabolism, NMR spectroscopy was performed. For this assay HUVECs were exposed to  $^{12}\text{C}$ -glucose,  $^{13}\text{C}$ -glucose (9%  $^{13}\text{C}$ -glucose + 91%  $^{12}\text{C}$ -glucose) and  $^{13}\text{C}$ -lactate (20%  $^{13}\text{C}$ -lactate + 80%  $^{12}\text{C}$ -lactate), in the presence and absence of hypoxia (mimicked by  $\text{CoCl}_2$ ). First, we analyzed the supernatants and observed that the cells consumed low levels of glucose, probably due to the short time of incubation. Comparing the samples in normoxia versus hypoxia there was a decreased concentration of lactate in hypoxia, which is represented in the  $^{13}\text{C}$  spectrum of cells exposed to  $^{13}\text{C}$ -lactate (Figure 4. 1 A), showing a decrease of around 10%. Moreover, a difference in the histidine peaks was also noticed but it was an interference due to  $\text{CoCl}_2$ , given that  $\text{Co}^{2+}$  binds to this amino acid, which reflects in a decreased signal of free histidine in hypoxia. It was also noticed a difference in the 2-hydroxyisobutyrate peak, being decreased in hypoxia represented in the  $^1\text{H}$  spectrum of cells exposed to  $^{12}\text{C}$ -glucose (Figure 4. 1 B).



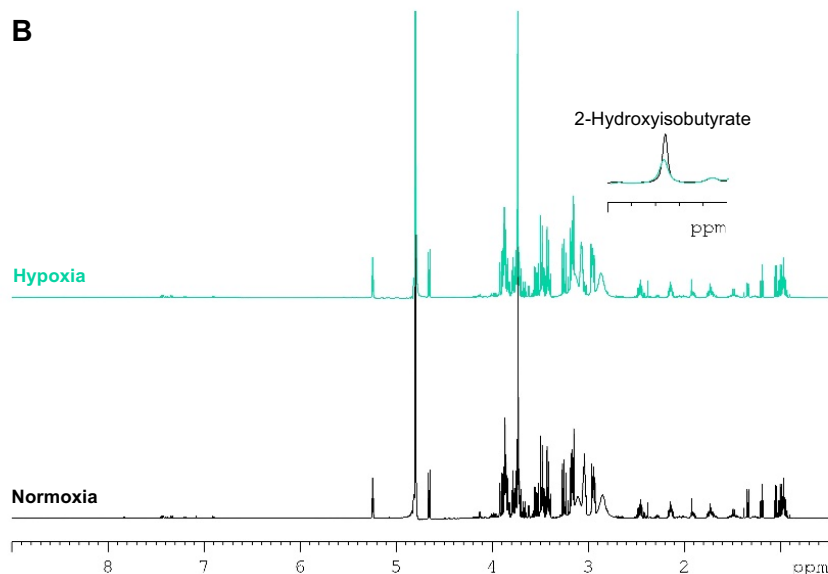


**Figure 4. 1 – NMR analysis of supernatants. (A)** Regions from the  $^{13}\text{C}$  spectrum of supernatants of cells exposed to  $^{13}\text{C}$ -lactate in normoxia (black line) and  $\text{CoCl}_2$ -induced hypoxia (green line). The amplified peaks correspond to the third position of lactate. **(B)** Spectral region from the 1D  $^1\text{H}$  NOESY experiment from  $^{12}\text{C}$ -glucose cell supernatants in normoxia (black) versus hypoxia (green). The amplified peak corresponds to 2-hydroxyisobutyrate.

Next we analyzed the aqueous phases, containing the intracellular polar and water-soluble metabolites. In spite of the low biomass found in the aqueous phase, it was possible to detect an increase of formate and a decrease of lactate, acetate and glucose in hypoxia in the  $^1\text{H}$  spectrum of cells exposed to  $^{13}\text{C}$ -lactate (Figure 4. 2). Another difference was detected at 3.75 ppm region, a metabolite that was also decreased in hypoxia, but it remained unknown since it was not found on the databases. In the case of  $^{13}\text{C}$ -lactate, only 3.4% of the lactate inside the cell (aqueous phase) was marked, which means that the intracellular lactate enters the cells, but it is also originated from other compounds.

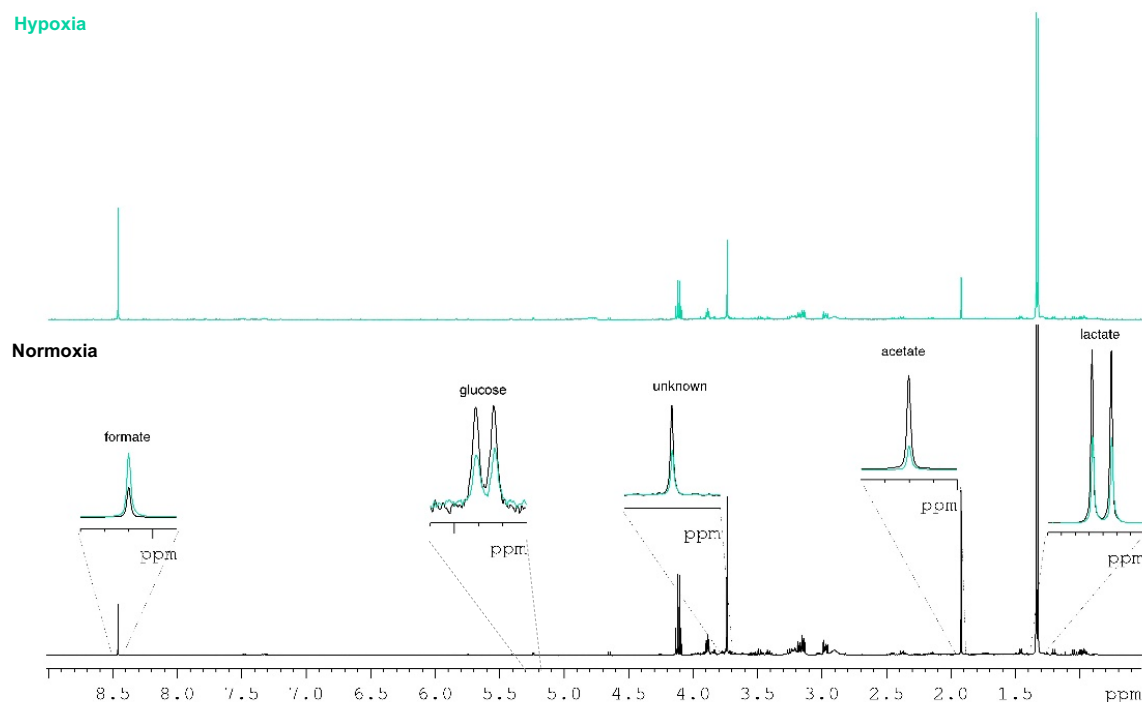
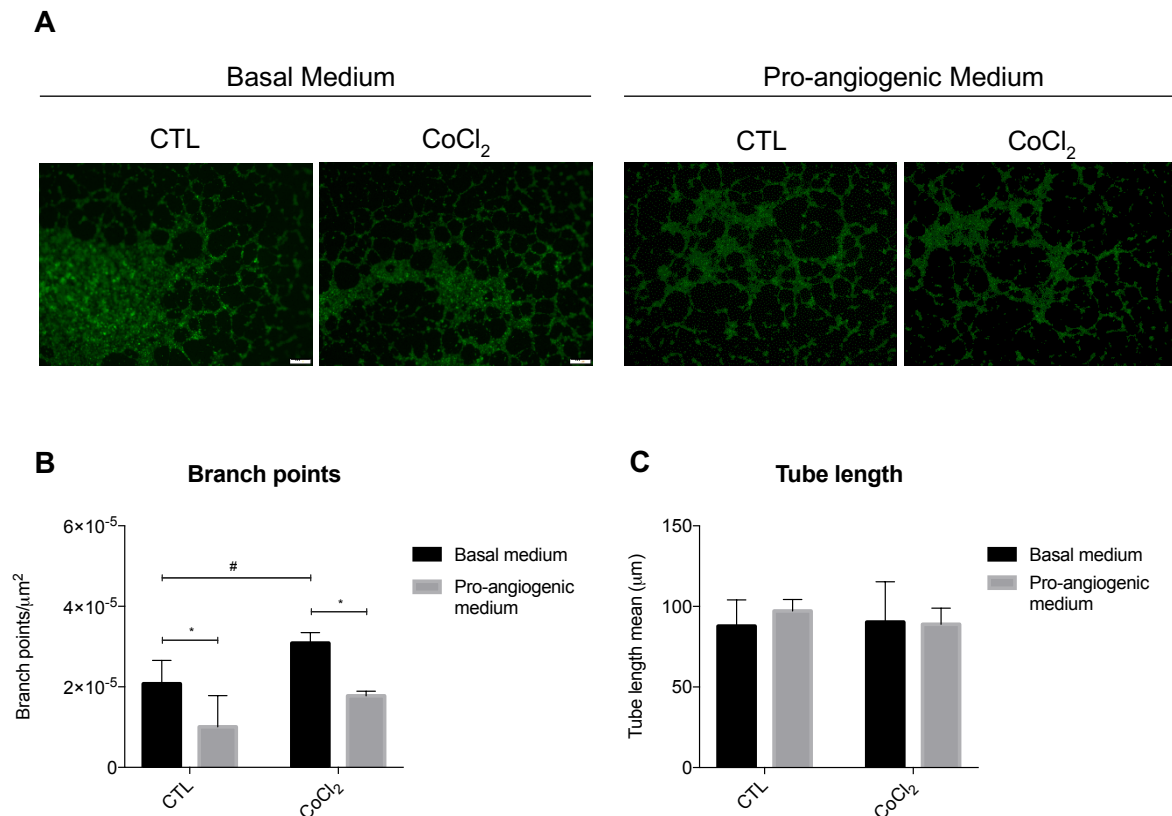


**Figure 4. 2 – NMR analysis of the aqueous phases.** Regions from the 1D  $^1\text{H}$  NOESY spectrum of intracellular content of cells exposed to  $^{13}\text{C}$ -lactate in normoxia (black line) and  $\text{CoCl}_2$ -induced hypoxia (green line). The amplified peaks correspond to formate, glucose, the unknown metabolite, acetate and lactate (left to right).

## 4.2. Influence of hypoxia in endothelial activation and vessel-like structures formation

To disclose the effect of hypoxia on tumor angiogenesis, *in vitro* tube forming assays were performed. HUVECs were exposed to 100  $\mu$ M  $\text{CoCl}_2$  (to mimic hypoxia) and added to matrigel-precoated plates for 6 h. These cells were cultured in two different supplemented media: a basal medium, only supplemented with FBS, and a pro-angiogenic medium, also supplemented with LSGS (a low serum with growth factors) and bFGF. Calcein-labeled HUVECs (Figure 4. 3 A) were observed after 6 h.  $\text{CoCl}_2$  exposition increased the number of branch points in both media (Figure 4. 3 B) comparing to the control (normoxia), even though the tube length mean didn't differ between treatments (Figure 4. 3 C). This suggest that hypoxia might potentiate the formation of vessel-like structures.

To confirm this result we performed an aortic ring assay, which is an *ex vivo* assay that consists in vessels sprouting from a segment of a rat aorta. The rings were embedded into matrigel and exposed to  $\text{CoCl}_2$  (present both in the medium and in the matrigel). Representative images of day 10 (Figure 4. 3 D) showed an inhibition of sprouting, which was confirmed by the decrease of branch points density normalized to the control (Figure 4. 3 E). This result contradicts the previous *in vivo* assay and what is described in the literature, since hypoxia was reported to potentiate angiogenesis.





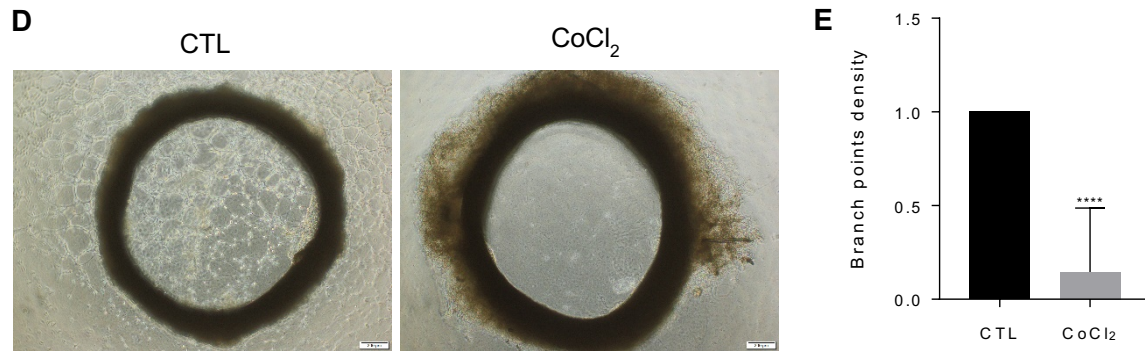


**Figure 4. 3 – Effect of hypoxia on the formation of vessel-like structures and sprouting.** (A) Representative images (40 x, scale: 200  $\mu$ m) of the vessel-like structures formed by calcein-labeled HUVECs. Cells were exposed to CoCl<sub>2</sub> and cultured in basal or pro-angiogenic medium. Quantification of the respective branch points (B) and tube length (C) of the newly-formed vessel-like structures. All data are represented as mean  $\pm$  SD. (\*)  $p < 0.05$ , Two-way ANOVA; (#)  $p < 0.05$ , Unpaired  $t$ -test. (D) Representative images of aortic rings at day 10 (40x, scale: 200  $\mu$ m) (E) Sprouting quantification: number of branch points per sprouting area (area around and inside the ring were sprouting was visible), normalized to the control. Results are represented as mean  $\pm$  SD. \*\*\*\* $p < 0.0001$ ; unpaired  $t$ -test (two-tailed).

ECs migration is a key process during sprouting angiogenesis. Therefore, we performed a wound healing assay, where HUVECs were exposed to CoCl<sub>2</sub> for 24 h (Figure 4. 4 A). There was a tendency to a decreased wound closure in ECs exposed to CoCl<sub>2</sub> comparing to the control (most noticed at 4 h and 6 h), although at the end of the assay the wound had closed (Figure 4. 4 B). Once again, this result goes against what is previously described, since hypoxia should have increased EC migration.

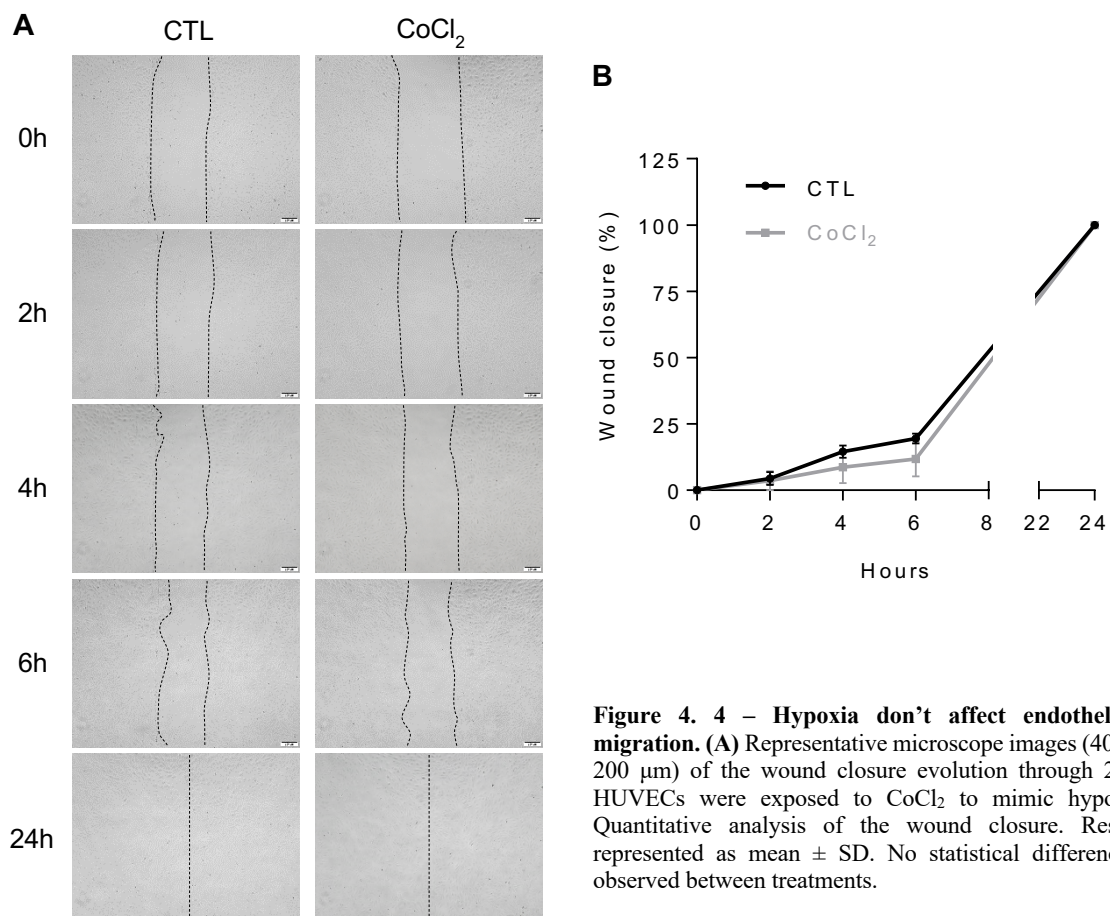


**Figure 4. 4 – Hypoxia don't affect endothelial cells migration.** (A) Representative microscope images (40 x, scale: 200  $\mu$ m) of the wound closure evolution through 24 hours. HUVECs were exposed to CoCl<sub>2</sub> to mimic hypoxia. (B) Quantitative analysis of the wound closure. Results are represented as mean  $\pm$  SD. No statistical differences were observed between treatments.

### 4.3. Effect of cysteine in endothelial activation under normoxia and hypoxia

Since Cys is a ROS scavenger important for the maintenance of redox equilibrium and high levels of ROS can be promoters of endothelial activation, we wanted to know the role of Cys in this process, under normoxia and hypoxia. Therefore, we performed an aortic ring sprouting assay (Figure 4. 5), in which segments from a rat aorta were exposed to Cys in normoxic and hypoxic conditions. There was a tendency to an increase of branch points density (Figure 4. 5 B), whether in normoxia or hypoxia. Moreover, the sprouting decreased when cells were exposed to Cys under hypoxia comparatively to normoxia. We also tested the effect of H<sub>2</sub>O<sub>2</sub> (ROS), which induced more aortic ring sprouting comparing to the control. Rings exposed to Cys and H<sub>2</sub>O<sub>2</sub> seemed to decrease the branch points density comparing to H<sub>2</sub>O<sub>2</sub> (not statistically significant) towards a similar level than rings exposed to Cys.

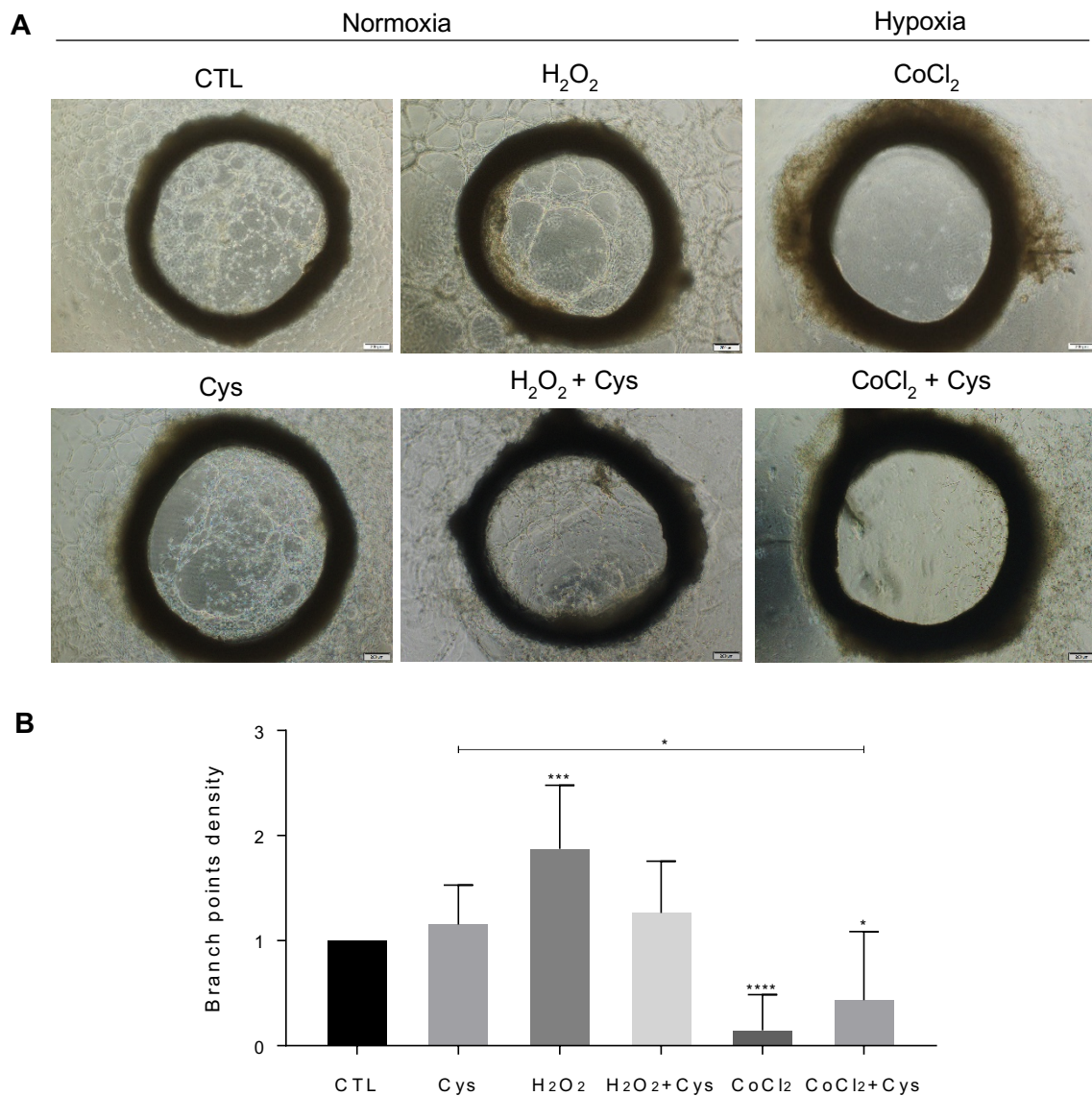


**Figure 4. 5 – Cystine effect on aortic ring sprouting.** (A) Representative images of rat aortic rings at day 10 (40x, scale: 200  $\mu$ m). The rat aorta segments were exposed to cysteine and H<sub>2</sub>O<sub>2</sub> under normoxic and/or hypoxic conditions. (B) Sprouting quantification: number of branch points per sprouting area (area around and inside the ring where sprouting was visible), normalized to the control. Results are represented as mean  $\pm$  SD. \* $p$ <0.05, \*\*\* $p$ <0.001, \*\*\*\* $p$ <0.0001; unpaired  $t$ -test (two-tailed).

Next, we performed a wound healing assay to determine the effect of Cys on endothelial cells migration. In Figure 4. 6, Cys didn't have an effect on cell migration. Cells under hypoxia with or without Cys had a smaller percentage of wound closure (most noticed at 6 h, Figure 4. 6 B) comparing to normoxia, without Cys influence. Moreover, H<sub>2</sub>O<sub>2</sub> exposition didn't affect cell migration, whether in the presence or absence of Cys.

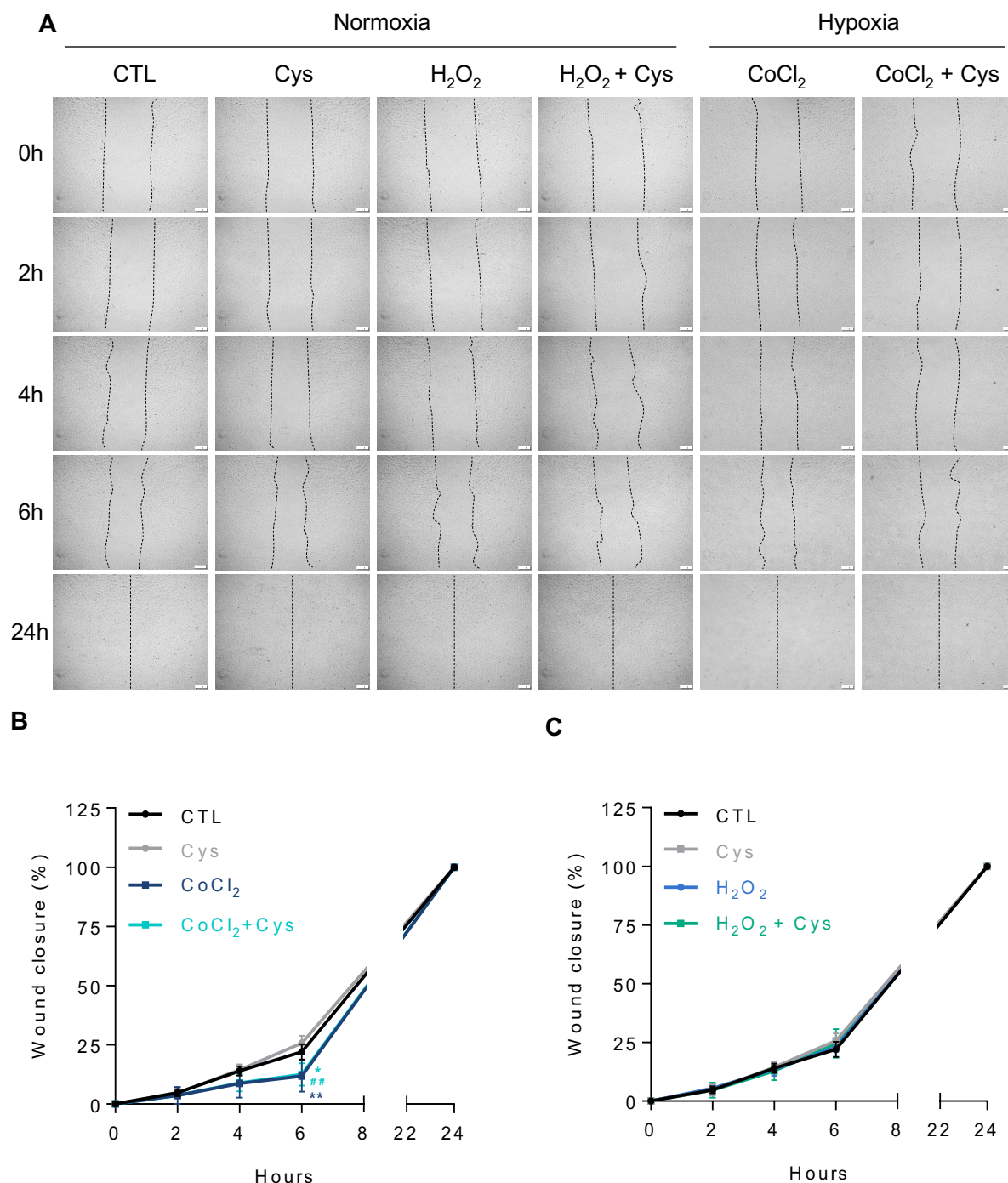


**Figure 4. 6 – Cysteine doesn't affect endothelial cells migration.** (A) Representative microscope images (40 x, scale: 200  $\mu$ m) of the wound closure evolution at 0h, 2h, 4h, 6h and 24h. HUVECs were exposed to cysteine under normoxia and hypoxia conditions and H<sub>2</sub>O<sub>2</sub>. (B) Quantitative analysis of the percentage of wound closure. Results are represented as mean  $\pm$  SD. \* $p$ <0.05, \*\* $p$ <0.01. (\*) statistical analysis in relation to the control; (#) statistical analysis in relation to Cys.

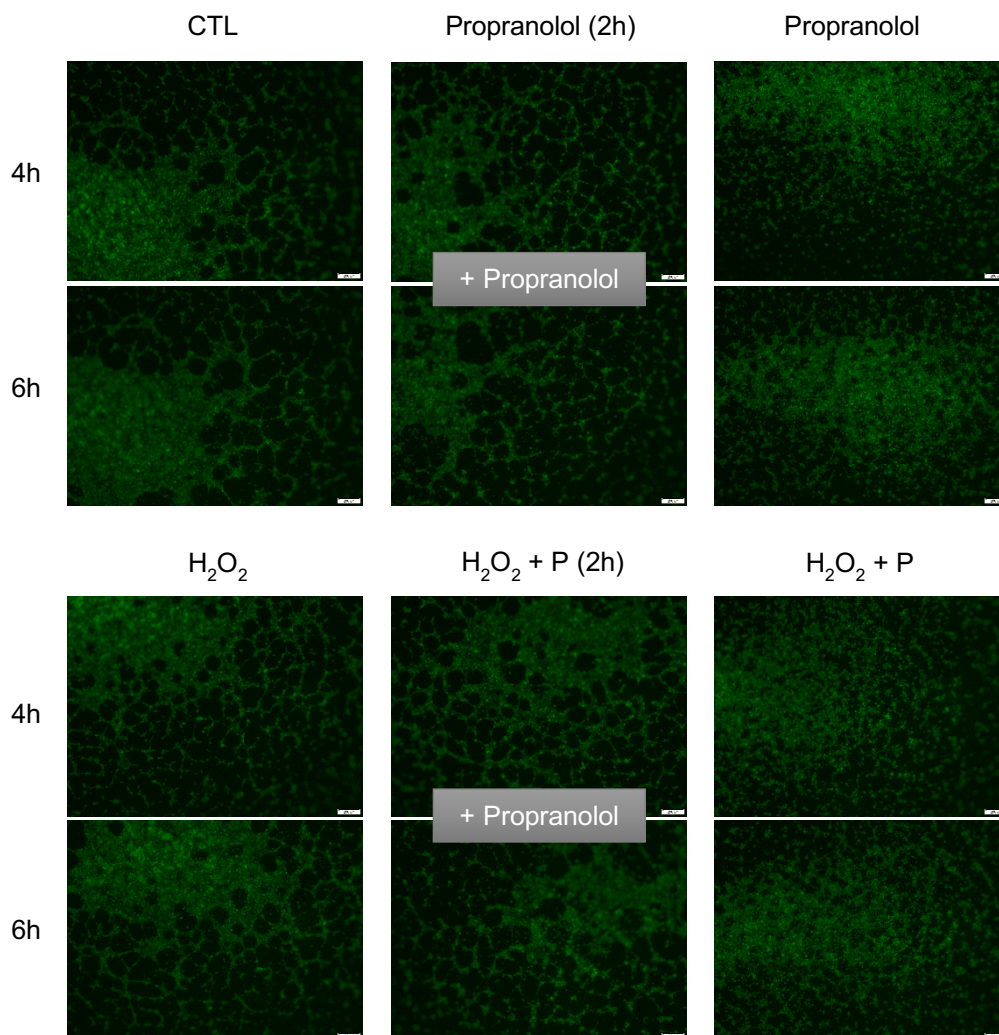


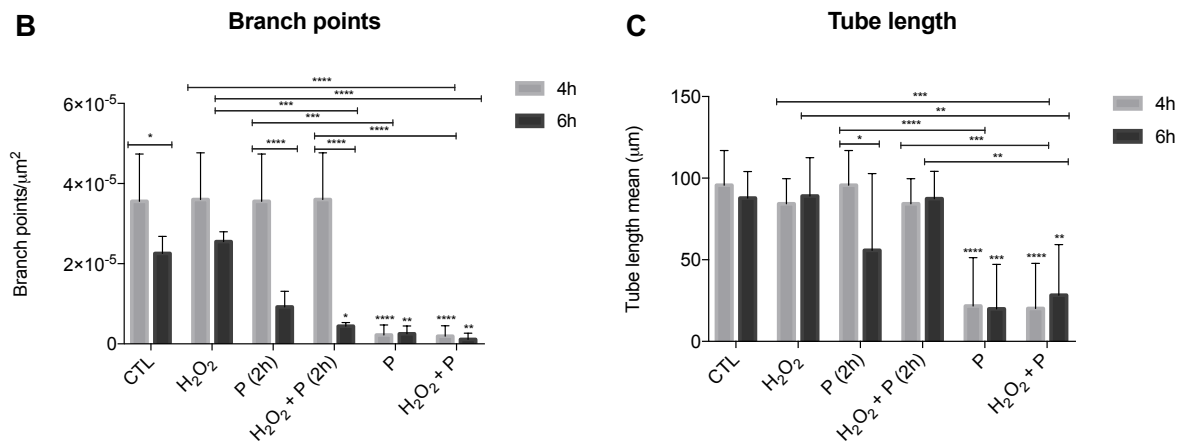
#### 4.4. Effect of propranolol in the formation of vessel-like structures

Since propranolol (P) promotes the regression of infantile hemangiomas by vasoconstriction, we started to study its effect on endothelial cell angiogenesis, by performing a tube forming assay (Figure 4. 7 and 8). HUVECs were added into matrigel-precoated plates and then exposed to 100  $\mu$ M propranolol and 15  $\mu$ M  $H_2O_2$  (to stimulate angiogenesis) for 6 h. Cells were also exposed to two different supplemented media: a basal and a pro-angiogenic medium.

Starting with basal medium (Figure 4. 7), the tube forming images obtained (A) showed that propranolol inhibited the formation of vessel-like structures and disrupted the already formed structures when added after 4 h (2 h of exposition, referred as Propranolol (2 h)). There was also a significant decrease in the number of branch points (B) and tube length (C) with propranolol comparing to the control. The number of branch points and tube length are two factors that help in the estimation of the extension of tube formation. Moreover, when propranolol was added after 4 h there was a significant decrease of number of branch points and tube length mean at 6 h.

##### A Basal Medium

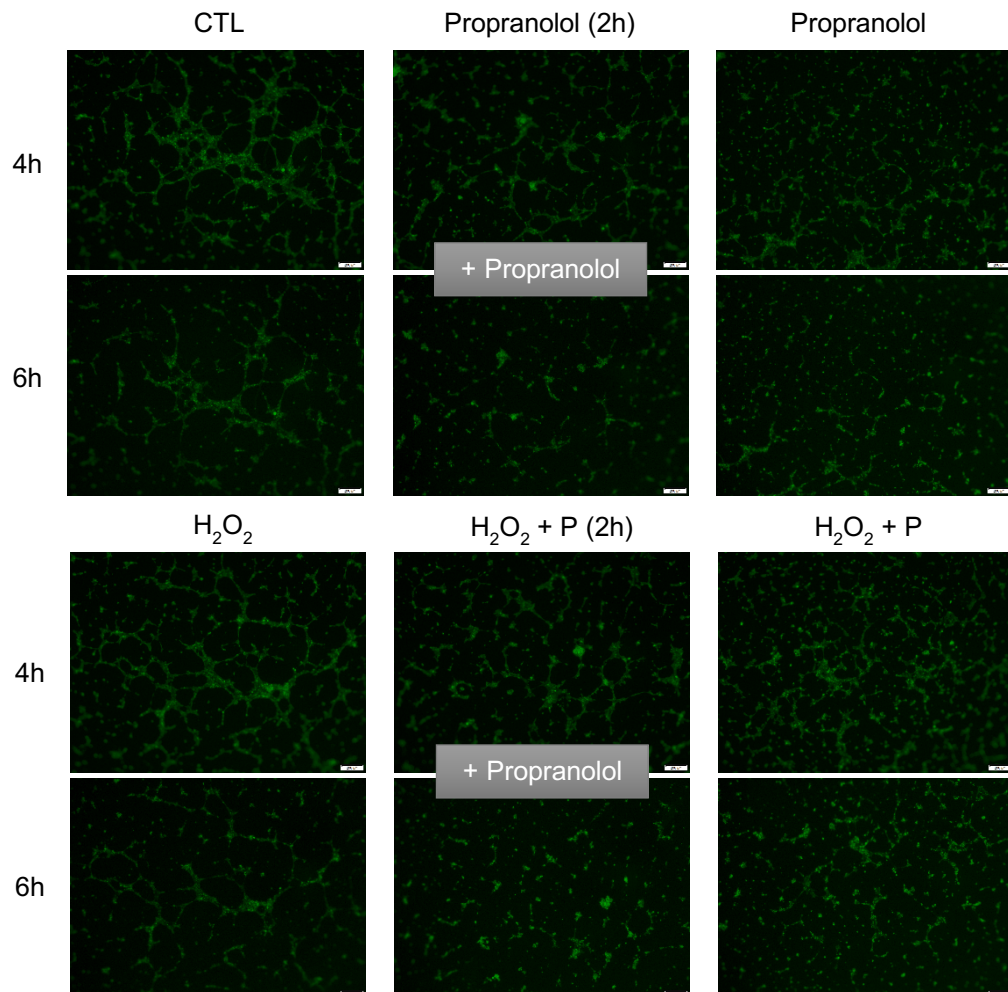




**Figure 4. 7 – Propranolol (P) inhibits the formation of vessel-like structures by HUVECs cultured in basal medium.** (A) Representative microscope images (40 x, scale: 200 µm) of the vessel-like structures formed by HUVECs after 4h and 6h. The number of branch points per area (B) and the tube length (C) were quantified in images from the whole well (40 x) under the microscope. All data are represented as mean ± SD. \* $p < 0.05$ , \*\* $p < 0.01$ , \*\*\* $p < 0.001$ , \*\*\*\* $p < 0.0001$ .

In the case of the pro-angiogenic medium (Figure 4. 8) it is visible that the net formed is wider than the one formed when cultured in basal medium. Similar to the last figure, propranolol disrupted most of the structures already formed and inhibited the formation of new vessel-like structures, which reflected in the decreasing number of branch points (Figure 4. 8 B) and tube length (Figure 4. 8 C) comparing to the control.

#### A Pro-angiogenic Medium



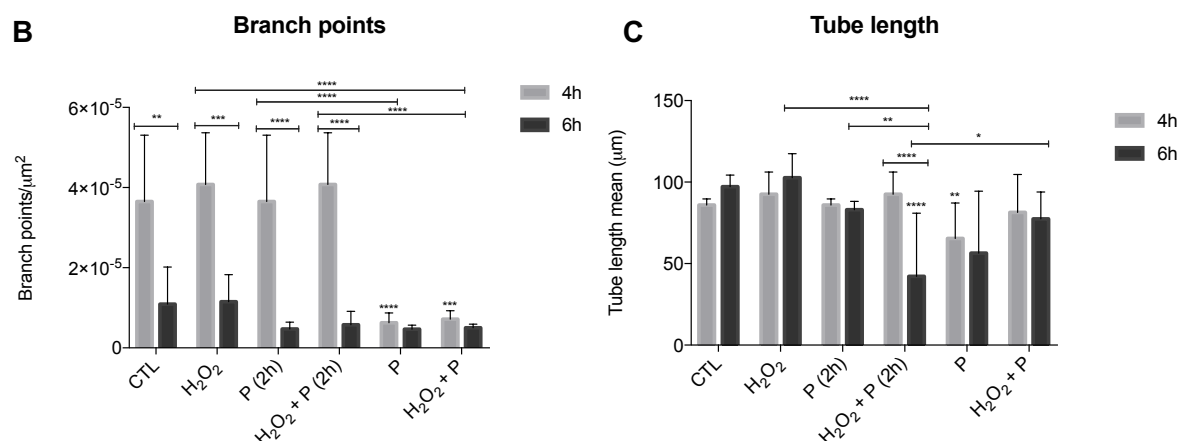


**Figure 4. 8 – Propranolol inhibits the formation of vessel-like structures by HUVECs cultured in pro-angiogenic medium.** (A) Representative microscope images (40 x, scale: 200 µm) of the vessel-like structures formed by HUVECs after 4h and 6h. The number of branch points per area (B) and the tube length (C) were quantified in images from the whole well (40 x) under the microscope. All data are represented as mean ± SD. \* $p < 0.05$ , \*\* $p < 0.01$ , \*\*\* $p < 0.001$ , \*\*\*\* $p < 0.0001$

#### 4.5. Propranolol effect on cell viability

To determine if propranolol had an effect on endothelial cells viability, a cell death analysis by flow cytometry was performed. In Figure 4. 9 the percentage of total cell death of HUVECs was not affected by propranolol, whether it was 2 h or 6 h of exposition. Moreover, the percentage of cell death due to necrosis, early and late apoptosis didn't present any differences between treatments (Supplementary Figure 1). Therefore, propranolol disrupts angiogenesis without compromising cell viability.

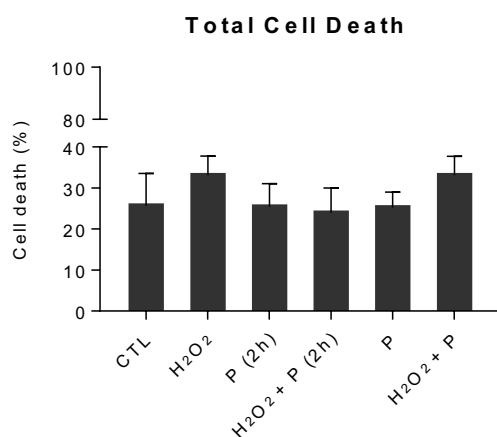


**Figure 4. 9 – Propranolol don't affect cell viability.** Cells were exposed for 6h to H<sub>2</sub>O<sub>2</sub>, Propranolol (for the last 2h and for the whole 6h) with or without H<sub>2</sub>O<sub>2</sub>. Results are shown as mean ± SD. No statistical differences were observed between treatments.

#### 4.6. Effect of propranolol on endothelial cell migration

The migration of endothelial cells is a crucial step during angiogenesis. In order to investigate the *in vitro* effects of propranolol in endothelial cells migration, a wound healing assay was carried out over 24 hours and monitored at the following timepoints: 0, 2, 4, 6, 8, 10 and 24 h. Both control and cells exposed to H<sub>2</sub>O<sub>2</sub> were able to completely close the wound, whereas cells exposed to propranolol were incapable of complete the wound closure at 24h (Figure 4. 10 A and C). Cells exposed to propranolol for less time (propranolol was only added in the last 4 h) had a similar wound closure range

of control and  $H_2O_2$  until the addition of propranolol, which promoted a decrease of the motility (Figure 4. 10 B). Therefore, propranolol inhibits the two-dimensional migration accessed by this assay.

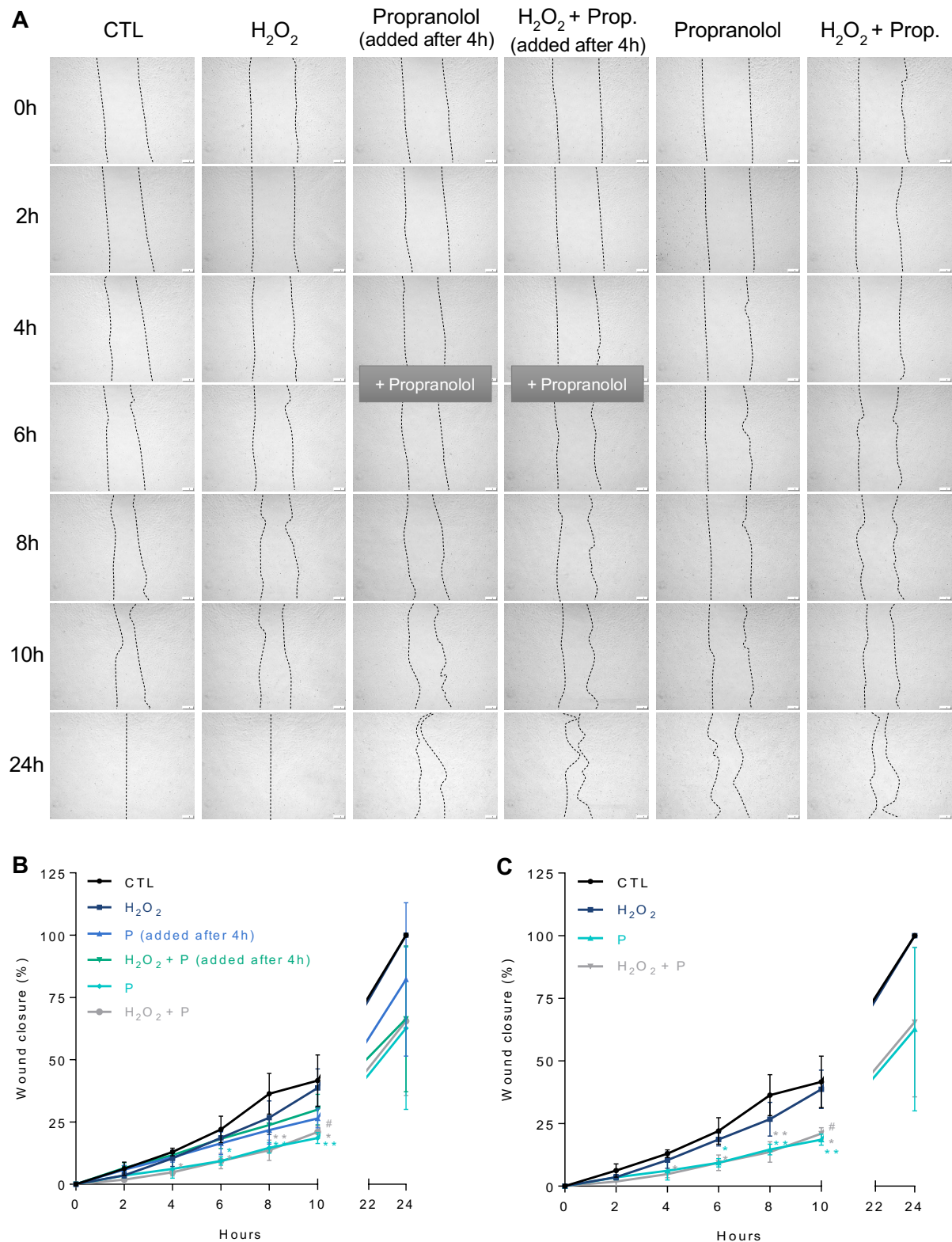


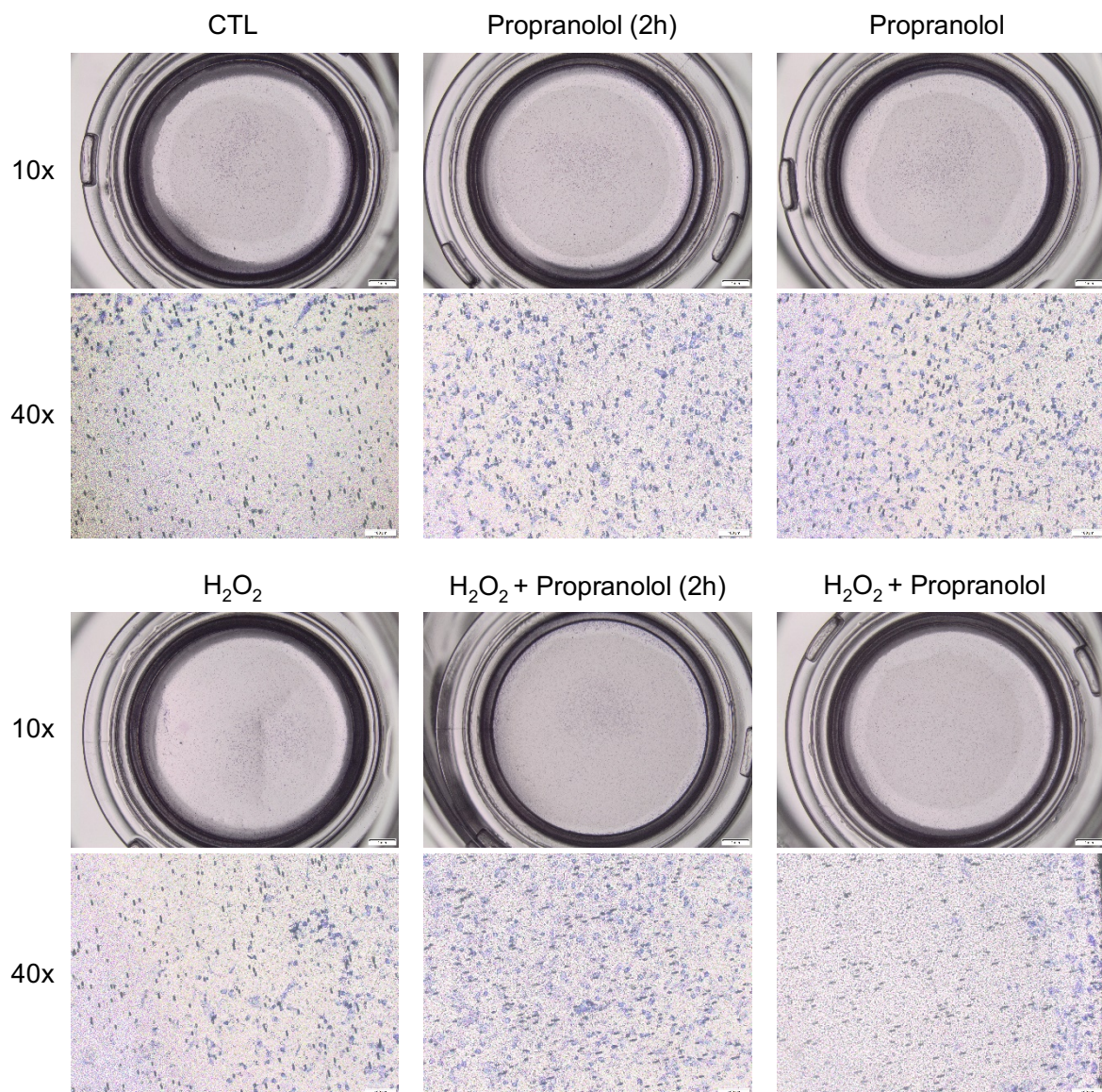
**Figure 4. 10 – Propranolol inhibits migration of endothelial cells. (A)** Representative microscope images (40 x, scale: 200  $\mu$ m) of the wound closure evolution through 24 hours. HUVECs were exposed to  $H_2O_2$  and propranolol with and without  $H_2O_2$ . **(B)** Quantitative analysis of the wound closure. **(C)** Quantitative analysis of the wound closure of only control,  $H_2O_2$ , propranolol and  $H_2O_2$ +propranolol. All results are represented as mean  $\pm$  SD. \* $p$ <0.05, \*\* $p$ <0.01. (\*) statistical analysis in relation to the control; (#) statistical analysis in relation to  $H_2O_2$ .



#### 4.7. Effect of propranolol on transwell migration

To further evaluate the directional migratory ability of HUVECs when exposed to propranolol, we performed a transwell migration assay. This technique allows the analysis of the ability of a single cell to migrate towards the bottom chamber, that is loaded with medium with serum in different conditions. Contrarily to the wound healing assay, we found no difference on cell transwell migration between treatments (Figure 4. 11).

**A**





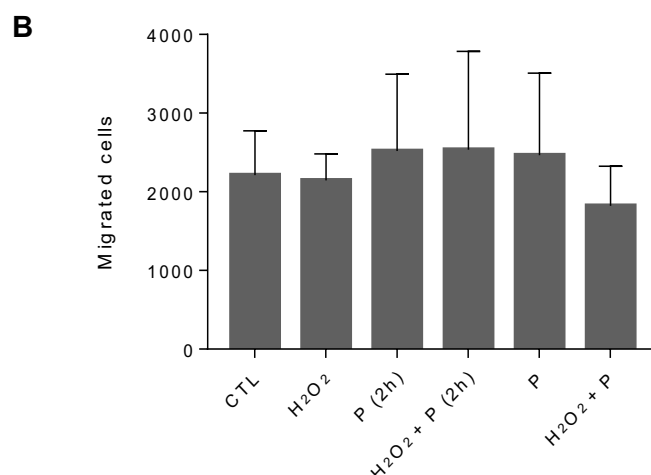


**Figure 4. 11 – Propranolol don't affect transwell migration.** (A) Representative images of HUVECs subjected to the transwell migration assay with the lower chamber loaded with serum-supplemented medium with the conditions. Top row: magnifier images of the transwell (10x, scale: 1 mm). Bottom row: microscopic images (100x, scale: 100  $\mu$ m). (B) Graphical representation of the migrated cells. Results are shown as mean  $\pm$  SD. No statistical differences were observed between treatments.

#### 4.8. Impact of Propranolol in ECs markers expression

To investigate if propranolol interferes with the expression of endothelial cell markers, an immunofluorescence staining was performed.

First, we analyzed the expression of two cell adhesion molecules (CAMs): ICAM (intercellular adhesion molecule, CD54) and VCAM (vascular cell adhesion molecule, CD106). ICAM is constitutively present on ECs while VCAM is weakly expressed,<sup>78</sup> although proinflammatory cytokines such as TNF $\alpha$  lead to an upregulation of both adhesion molecules.<sup>79,80</sup> These molecules are crucial for the leukocyte transendothelial migration out of blood vessels.<sup>78</sup> In Figure 4. 12, both molecules presented the same expression dynamic. H<sub>2</sub>O<sub>2</sub> and P (2 h) stimulated an upregulation of these molecules (Figure 4. 12 B).

Furthermore, we analyzed the expression of CD146 and vWF, two EC markers. CD146 is also a CAM, involved in cell-cell adhesions.<sup>81</sup> Besides, vWF (von Willebrand factor) has a principal role in hemostasis.<sup>82</sup> In Figure 4. 13 B, Propranolol downregulated the CD146 expression, while P (2 h) upregulated. In the case of vWF (Figure 4. 13 C) there was also a tendency to downregulation when exposed to propranolol.

On all four EC markers, a shorter exposition to propranolol induced an upregulation of the respective marker, while propranolol for the whole 6h had the opposite effect. This could indicate that the expression of these EC markers is affected by propranolol in a time-dependent manner.

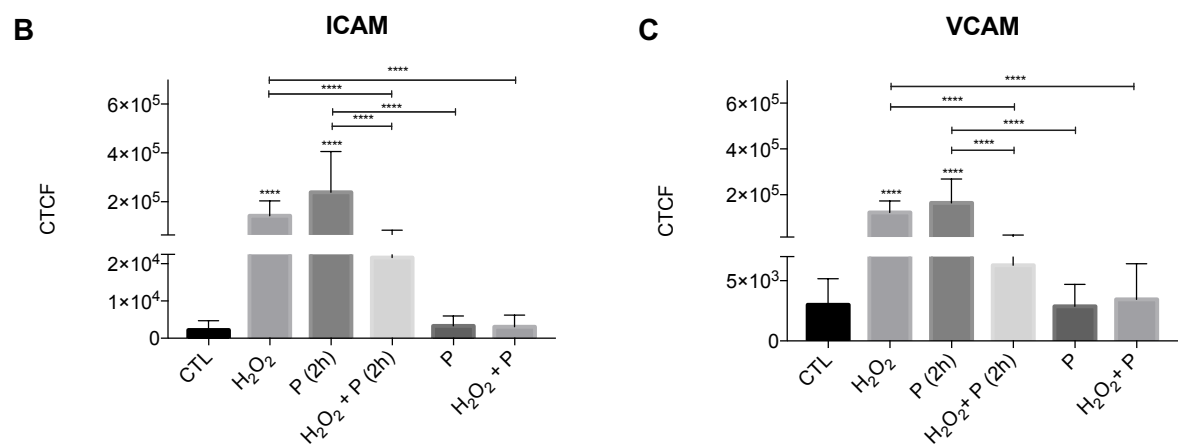
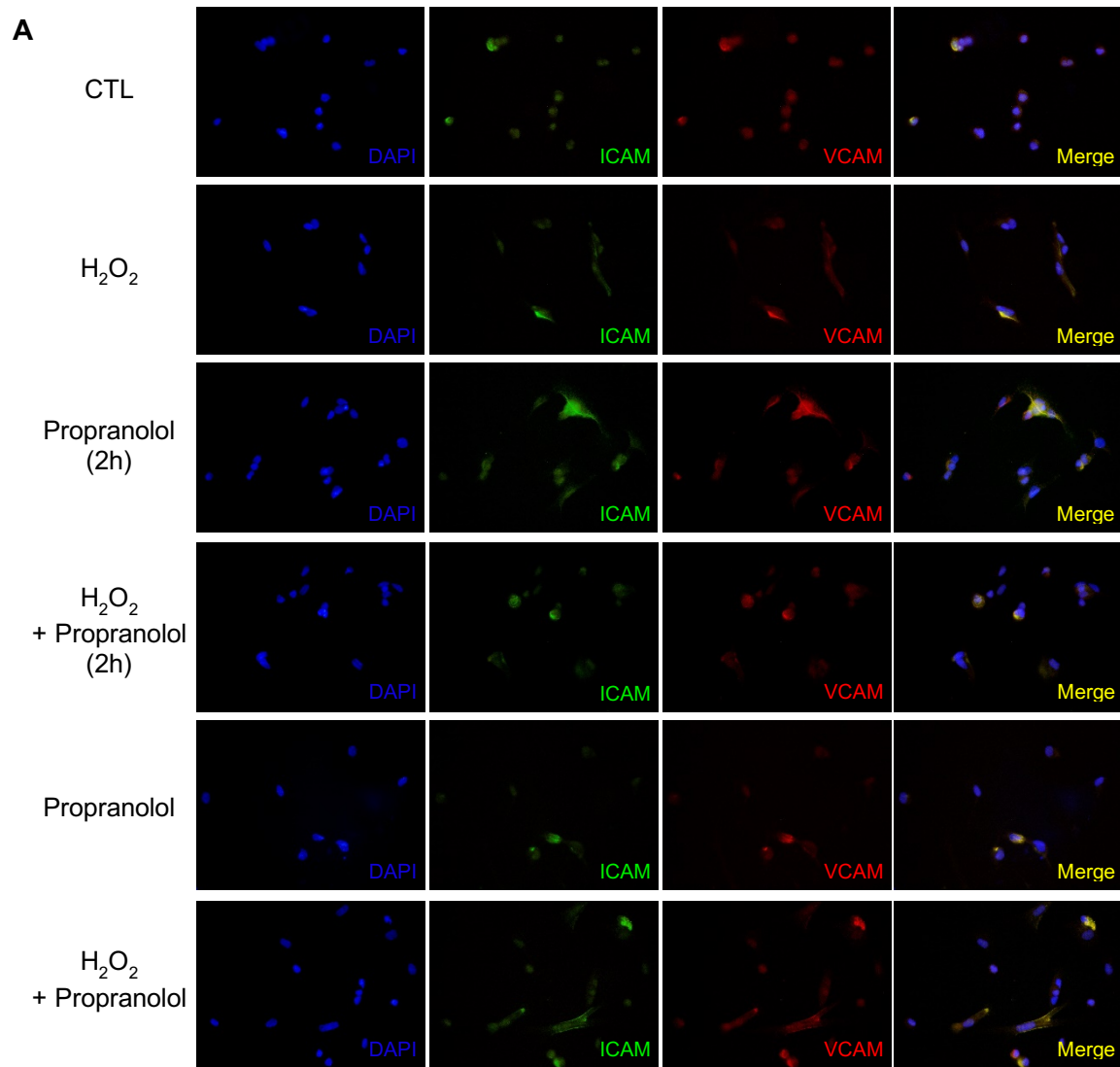


**Figure 4. 12 – ICAM and VCAM expression in HUVECs. (A)** Immunofluorescence images (amplification 400x). Cell nuclei were stained with DAPI (blue), ICAM expression is indicated by green fluorescence, red fluorescence is VCAM, and the merge of ICAM and VCAM as yellow. **(B)** Quantification of ICAM and **(C)** VCAM expression by CTCF (corrected total cell fluorescence). All data are represented as mean ± SD. \* $p < 0.05$ , \*\* $p < 0.01$ , \*\*\* $p < 0.001$ , \*\*\*\* $p < 0.0001$ .

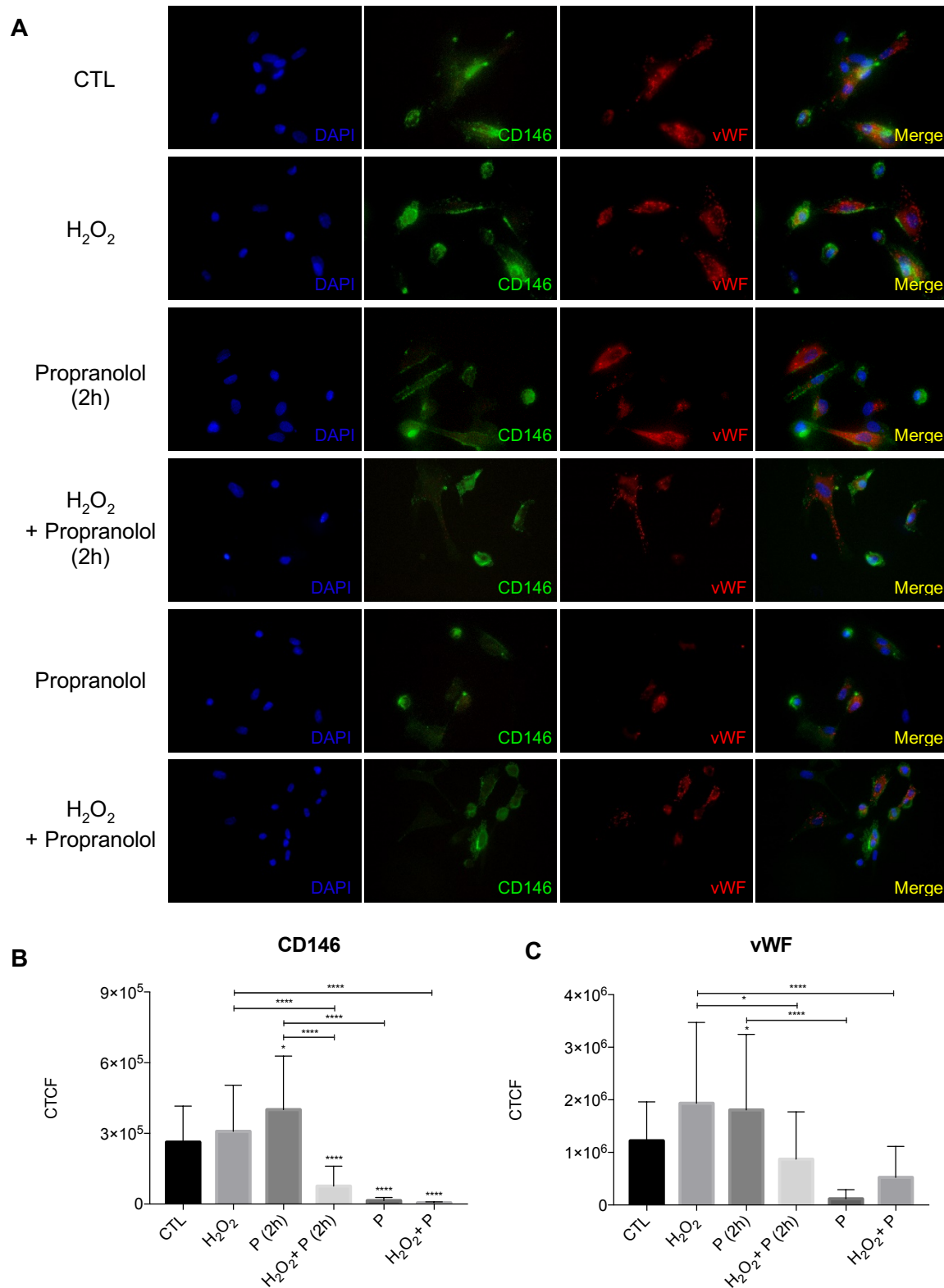


**Figure 4. 13 – CD146 and vWF expression in HUVECs.** (A) Immunofluorescence images (amplification 400x). Cell nuclei were stained with DAPI (blue), CD146 expression is indicated by green fluorescence, red fluorescence is vWF, and the merge as yellow. (B) Quantification of CD146 and (C) vWF expression by CTCF (corrected total cell fluorescence). All data are represented as mean  $\pm$  SD. \* $p$ <0.05, \*\* $p$ <0.01, \*\*\* $p$ <0.001, \*\*\*\* $p$ <0.0001.

#### 4.9. Effect of propranolol in *ex vivo* sprouting

In order to diminish the bridge between *in vitro* and *in vivo* studies, the aortic ring assay emerged as an *ex vivo* technique to analyze angiogenesis. The aortic rings were embedded in matrigel and exposed to propranolol, H<sub>2</sub>O<sub>2</sub> and the combination of both (Figure 4. 14). H<sub>2</sub>O<sub>2</sub> induced more sprouting comparing to the control, forming vessel-like structures (Figure 4. 14 A), which reflected in an increase of the branch points density (Figure 4. 14 B). On the contrary, propranolol impeded sprouting, in the presence or absence of H<sub>2</sub>O<sub>2</sub>, which corroborated the previous results obtained *in vitro*.

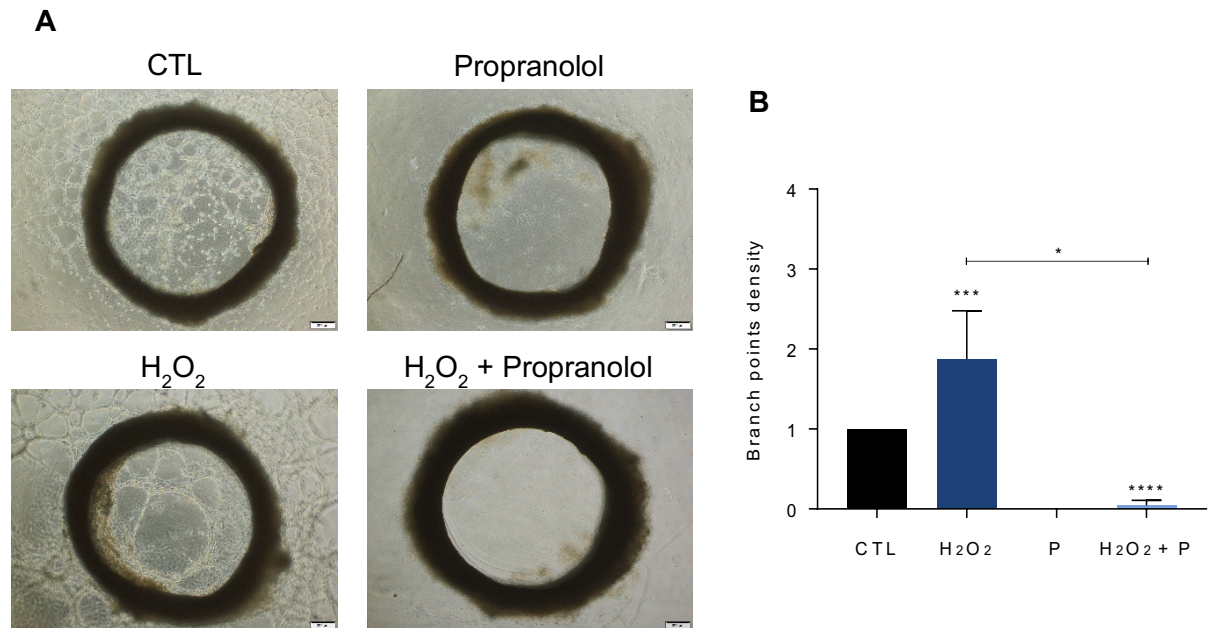


**Figure 4. 14 – Propranolol inhibits aortic ring sprouting.** (A) Representative images of aortic rings embedded in matrigel (40x, scale: 200  $\mu$ m) (B) Sprouting quantification: number of branch points per sprouting area (area around and inside the ring were sprouting was visible), normalized to the control. Results are represented as mean  $\pm$  SD. \* $p$ <0.05, \*\* $p$ <0.01, \*\*\* $p$ <0.001, \*\*\*\* $p$ <0.0001; unpaired  $t$ -test (two-tailed).

#### 4.10. Metabolic remodeling of endothelial cells – *ex vivo* model

In order to understand the metabolic remodeling involved during sprouting, aortic rings were collected after the sprouting assay. Then, we performed an NMR analysis of the rings exposed to the conditions mentioned in this thesis: CoCl<sub>2</sub>, cysteine (Cys), CoCl<sub>2</sub> + Cys, H<sub>2</sub>O<sub>2</sub>, propranolol (P) and H<sub>2</sub>O<sub>2</sub>+P. In Figure 4. 15 are the metabolites found in at least three conditions.

In this set are metabolites connected by metabolic pathways. For instance, isoleucine, leucine and valine (A) are amino acids belonging to the same biosynthesis and degradation pathways. These metabolites were in higher levels in rings exposed to propranolol (P) and H<sub>2</sub>O<sub>2</sub>+P comparing to the control, being the levels of leucine and valine in H<sub>2</sub>O<sub>2</sub>+P superior to the ones found in propranolol and H<sub>2</sub>O<sub>2</sub> exposed rings. While isoleucine and leucine were absent in the hypoxia spectrum, valine was present in hypoxia but not in normoxia. 3-hydroxyisovalerate (H) is also present in this pathway, downstream leucine. Similar to valine, this metabolite presented higher levels in hypoxia comparing to normoxia. Cys and H<sub>2</sub>O<sub>2</sub>+P also induced a higher level of 3-hydroxyisovalerate, comparing to the control. Glutamine (A) and the previous amino acids are associated to aminoacyl-tRNA biosynthesis, a major pathway during translation. Similarly, P and H<sub>2</sub>O<sub>2</sub>+P exposition resulted in an increased level of

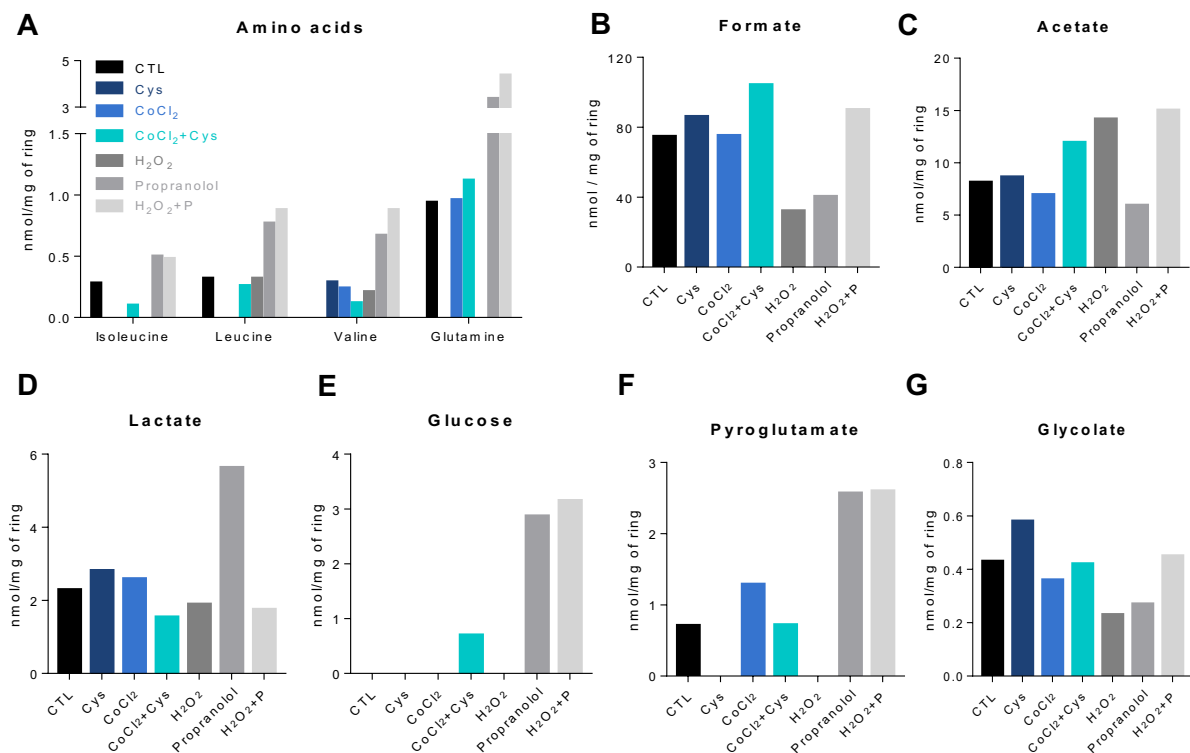
glutamine. This suggests that propranolol might induce the expression of these molecules to increase translation.

There are metabolites involved in pyruvate metabolism: formate (B), acetate (C) and lactate (D). Rings exposed to Cys had increased levels of these metabolites comparing with the control. However, rings exposed to  $\text{CoCl}_2$ +Cys had higher levels of formate and acetate comparing to the control,  $\text{CoCl}_2$  and Cys. Regarding propranolol, only lactate was increased comparing to the control. Besides, the rings exposed to  $\text{H}_2\text{O}_2$ +P had higher levels of formate and acetate comparing to control,  $\text{H}_2\text{O}_2$  and propranolol, while lactate had a decreased expression in  $\text{H}_2\text{O}_2$ +P comparing to these conditions.

Acetate (C), lactate (D) and glucose (E) are integrated in the glycolysis and gluconeogenesis pathways. Referring to glycolysis, glucose is upstream, while lactate and acetate are downstream of pyruvate. Glucose wasn't detected in CTL,  $\text{CoCl}_2$ , Cys and  $\text{H}_2\text{O}_2$ , yet it was observed an increased level on  $\text{H}_2\text{O}_2$ +P exposed ring comparing to propranolol. The absence of glucose and presence of lactate and acetate may indicate an induction of glycolysis in rings exposed to Cys,  $\text{CoCl}_2$  and  $\text{H}_2\text{O}_2$ .

Formate (B) and glycolate (G) belong to glyoxylate and dicarboxylate metabolism, being glycolate upstream and formate downstream of glyoxylate. In the case of formate, Cys exposed rings presented lower levels than  $\text{CoCl}_2$ +Cys, while the glycolate dynamic was the opposite. Both propranolol and  $\text{H}_2\text{O}_2$  decreased the expression of glycolate and formate.

The remaining metabolites were not included in the mentioned pathways. Choline (J) is integrated in glycine, serine and threonine metabolism and presented higher levels in aortic rings exposed to Cys and propranolol. Pyroglutamate (F) is integrated in GSH metabolism, such as Cys. This metabolite reached higher levels in  $\text{CoCl}_2$ , P and  $\text{H}_2\text{O}_2$ +P. At last, dimethylamine (I) belongs to carbon and also methane metabolism, reaching lower levels than the control in all conditions.



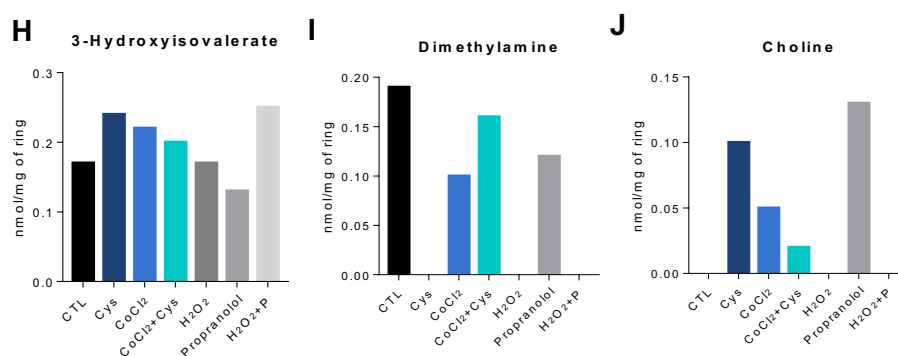


**Figure 4. 15 – Metabolites from aortic rings identified by NMR analysis.** The aortic rings were collected after the sprouting assay and analyzed by NMR. Metabolites found: (A) Amino acids: isoleucine, leucine, valine and glutamine; (B) formate; (C) acetate; (D) lactate; (E) glucose; (F) pyroglutamate; (G) glycolate; (H) 3-hydroxyisovalerate; (I) dimethylamine and (J) choline. Y axis: nanomoles per mg of ring tissue.

## 5. Discussion

It is stated that the tumor microenvironment promotes angiogenesis, in order to satisfy the cancer cells' needs.<sup>17,83</sup> Pro-angiogenic molecules are mainly produced by tumor cells, which modulate ECs metabolism.<sup>84</sup> When rapid tumor growth occurs, the blood supply becomes insufficient leading to a hypoxic tumor microenvironment. The oxygen deprivation stimulates the stabilization of the transcription factor HIF-1 $\alpha$ ,<sup>52</sup> promoting the activation of pro-angiogenic genes, such as VEGF.<sup>12</sup>

Since hypoxia has a high impact in angiogenesis, the first objective of the present work was to disclose the role of hypoxia in the metabolic remodeling during the endothelial cell activation. Hence, we first verify the impact of hypoxia mimicked by CoCl<sub>2</sub> in EC metabolism by NMR. We found that lactate levels were decreased in hypoxia both in the extra- and intracellular milieu (Figure 4. 1 A and Figure 4. 2), comparing to normoxia. Lactate is known to act as a pro-angiogenic molecule by interfering with PHD 2, thus activating HIF-1 $\alpha$ , or by activation of the NF- $\kappa$ B pathway.<sup>85</sup> Regardless, it was expected that the extracellular lactate levels were higher in hypoxia, since hypoxia upregulate glycolysis and consequently the secretion of lactate.<sup>86</sup> Moreover, 2-hydroxyisobutyrate was found in higher levels in the supernatant of cells cultured in hypoxia (Figure 4. 1 B). This metabolite is associated with the valine, leucine and isoleucine degradation pathway.<sup>87</sup> The increase of intracellular formate levels in hypoxia (Figure 4. 2) may reveal a proliferating phenotype, since formate is involved in the purine synthesis on proliferating cells, contributing to the one carbon metabolism demand.<sup>88</sup> Comparatively, the intracellular levels of glucose, lactate and acetate decreased (Figure 4. 2), which may indicate an energy production by oxidative phosphorylation, since they all can be precursors of pyruvate. Therefore, the data obtained seems to indicate a proliferative phenotype of cells exposed to hypoxia, although it's necessary to repeat this assay to validate this result. Nevertheless, the low exposure time and low concentration of <sup>13</sup>C-glucose may have contributed to the overall low resonance signal obtained.

Concerning endothelial activation, we exposed HUVECs to CoCl<sub>2</sub> and found that hypoxia increased the number of branch points, thus promoting the formation of vessel-like structures (Figure 4. 3 A-C). This is in accordance with the information found in the literature, since hypoxia is known to stimulate angiogenesis. However, the *ex vivo* rat aortic rings exposed to CoCl<sub>2</sub> presented an inhibition of sprouting comparing to normoxia (Figure 4. 3 D-E). Also, HUVECs exposed to CoCl<sub>2</sub> had a decreased wound closure percentage comparing to the control (Figure 4. 4). This make us question if the

concentration of CoCl<sub>2</sub> used is actually mimicking hypoxia. Despite chemically CoCl<sub>2</sub> reacts with oxygen impairing its dissolution and oxygenation of aqueous solutions,<sup>89</sup> CoCl<sub>2</sub> also stabilizes HIF-1 $\alpha$ , by interfering with the activity of PHDs.<sup>90</sup> Cobalt is known as a hypoxia mimicking agent both *in vivo*<sup>91</sup> and in cell culture, altering several systemic mechanisms related to hypoxia<sup>92–94</sup>, namely the stimulation<sup>54</sup> and stabilization of HIF-1 $\alpha$ , thus preventing its degradation.<sup>95</sup> Although it is widely used in cellular experiments due to its low-cost and no special culture and handle conditions, there are some limitations in this model. Results from high density oligonucleotide arrays performed on Hep3B cell line (hepatocellular carcinoma) showed that CoCl<sub>2</sub>-induced hypoxia promoted the transcription of gene sets that were not affected by low oxygen-induced hypoxia (1% O<sub>2</sub>).<sup>96</sup> Besides, Chandel *et al.* showed that CoCl<sub>2</sub> also stimulated ROS generation via a mitochondria-independent mechanism, which in turn leads to the activation of HIF-1-dependent transcription. However, this implies that pathways not related to hypoxia can be activated by the ROS produced.<sup>97</sup> Under these circumstances, CoCl<sub>2</sub> needs to be further analyzed because it can reproduce some of the effects generated by oxygen deprivation. Moreover, a study from Aplin *et al.* showed that aortic rings cultured in collagen gels under a reduction of O<sub>2</sub> levels (1–4%) resulted in inhibition of the angiogenic sprout, since hypoxia caused aortic rings to become unresponsive to exogenous VEGF.<sup>98</sup> This explains the differences observed in the *in vitro* and *ex vivo* studies.

Recently our team showed the relevance of thiols (including Cys) in cancer cell remodeling and chemoresistance.<sup>53,54</sup> Cys is one component of GSH, an important ROS scavenger for the maintenance of redox equilibrium,<sup>99</sup> which have being pointed as an inhibitor of angiogenesis.<sup>100</sup> Since ROS act as pro-angiogenic molecules, we had the intent to investigate the effect of Cys in endothelial activation. Although Cys didn't affect *in vitro* migration (Figure 4. 6), there was a tendency for a sprouting increase in the *ex vivo* aortic rings (Figure 4. 5), whether in normoxia or hypoxia. Also, HUVECs exposed to Cys and H<sub>2</sub>O<sub>2</sub> (ROS) had the same wound closure range of control (Figure 4. 6 C). However, aortic rings exposed to H<sub>2</sub>O<sub>2</sub> presented a higher branch points density comparing to control, but these levels decreased when Cys was added. This suggests that ROS may play a role in inducing angiogenesis, being this effect reverted when Cys is added. As a ROS scavenger, Cys leads to a decrease of free H<sub>2</sub>O<sub>2</sub>, inhibiting ROS-induced angiogenesis. Other studies also corroborate that antioxidants, including thiols, decrease the angiogenic rate (reviewed by Radomska-Leśniewska *et al.*<sup>101</sup>). Kubota *et al.* investigated the angiogenic response after alkali injury of the cornea, showing that pretreatment with NAC (N-acetyl-L-Cys) significantly reduced corneal angiogenesis by downregulating the NF- $\kappa$ B pathway in both SOD-1-deficient and wild-type mice.<sup>102</sup> In another study by Agarwal *et al.*, NAC therapy in athymic nude mice with MDA-MB-435 xenografts induced endothelial cell apoptosis and reduction of microvascular density, leading to tumor cell apoptosis.<sup>103</sup>

In the last years propranolol, a non-selective  $\beta$ -blocker, was applied to hemangiomas treatment. This drug was used for symptoms like hypertension, myocardial alterations or migraine and was accidentally discovered<sup>104</sup> to be a promising treatment for infantile hemangioma (IH), mainly treated with corticosteroids. Since then, several studies have shown the regression of IH tumors after propranolol treatment, with less adverse effects than corticosteroids.<sup>60</sup> Despite its effectiveness, the mechanism behind propranolol needs further investigation. Therefore, our next objective was to determine the effect of propranolol on angiogenesis. The tube forming assay showed that propranolol inhibited the formation of vessel-like structures and disrupted vessel-like structures (Figure 4. 7 and 8). We cultured HUVECs in two different mediums, designated basal and pro-angiogenic medium, to mimic different tumor microenvironments: one with lower levels of pro-angiogenic molecules and other rich in pro-angiogenic molecules. Next we performed a flow cytometry cell death analysis that showed that propranolol didn't affect cell viability (Figure 4. 9), excluding the induction of cell death as a mode of action. Regarding migration, a critical event for new vessel sprouting, propranolol inhibited two-



dimensional migration (Figure 4. 10), whereas the directional migration through a transwell (Figure 4. 11) was not affected. Lamy *et al.* showed in a similar assay that propranolol inhibited HUVECs migration in a dose-dependent manner.<sup>105</sup> Contrarily to our protocol, they added a growth factor-enriched media 2 h after the cells addition to the upper chamber, to stimulate cell migration.

To complete our propranolol study *in vitro*, the expression of some endothelial markers was assessed by immunofluorescence (IF). H<sub>2</sub>O<sub>2</sub> and P (2 h) lead to an upregulation of ICAM and VCAM (Figure 4. 12), whereas cells exposed to propranolol during the whole exposition time didn't show a differential expression. Which seems that propranolol may abrogate the endothelial activation by ROS, but by itself propranolol does not affect the activation of endothelial cells. In the case of CD146 and vWF, exposition to propranolol resulted in a downregulated expression, while P (2 h) had the opposite effect (Figure 4. 13).

To close the propranolol chapter, an aortic ring sprouting assay was performed (Figure 4. 14), corroborating the result obtained *in vitro*: propranolol inhibited sprout. However, H<sub>2</sub>O<sub>2</sub> induced sprouting of the aortic rings, contrarily to the assays performed *in vitro* in which it didn't seem to have an effect. As a ROS, H<sub>2</sub>O<sub>2</sub> has a short life inside the cell, which could reflect in the absence of effect in the *in vitro* assays. According to literature ROS are associated with stimulation of angiogenesis. Moreover, in the sequence of the work developed by a PhD student from our team, monocytes exposed to H<sub>2</sub>O<sub>2</sub> acquire an endothelial phenotype. Importantly, we cannot forget that an aortic ring resumes the vessels microenvironment, since it has all the cell types that constitute blood vessels organized in a vessel structure. Therefore, the response to sprouting stimuli will be processed in a more efficient way by endothelial cells within an aortic ring than by a pure endothelial cell population as HUVECs.

With the intent to understand the metabolic remodeling involved during sprouting, the rings were analyzed by NMR after the sprouting assay (Figure 4. 15). Metabolites were analyzed according to the metabolic pathway in which they belong. Isoleucine, leucine and valine are a group of amino acids, designated branched-chain amino acids (BCAA). A study showed that BCAA increased eNOS expression and ROS production in ECs,<sup>106</sup> which shows the importance of these metabolites in the angiogenesis context. Moreover, the presence of acetate and lactate and the glucose absence suggest an induction of glycolysis in rings exposed to Cys, CoCl<sub>2</sub> and H<sub>2</sub>O<sub>2</sub>. Stimulation of glycolysis on ECs by hypoxia was also showed by Cantelmo *et al.*. They isolated endothelial cells from mice livers with tumors originated by B16-F10 melanoma cells and used liquid chromatography-mass spectrometry (LC-MS), showing that hypoxia increased glycolysis.<sup>107</sup> Additionally, formate and glycolate belong to glyoxylate and dicarboxylate metabolism and while higher levels of formate were observed in CoCl<sub>2</sub>+Cys exposed rings, higher levels of glyoxylate were observed upon exposure to Cys. Nevertheless, these results correspond to rings of a single individual. Currently, more samples from different animals are being analyzed.

## 5.1. Main conclusions

In this thesis we showed that hypoxia alters metabolic pathways that can be important to tumor angiogenesis, giving some insights of what happens in the tumor microenvironment. Moreover, we analyzed the role of Cys in endothelial activation, showing *ex vivo* that it can be a promising strategy to disturb angiogenesis. Finally, we determined the effect of propranolol *in vitro* and *ex vivo*, suggesting it can be a potential therapeutic agent for tumor angiogenesis, although it needs to be better studied in this context.



## 5.2. Future perspectives

- To test different hypoxic conditions as different concentrations of CoCl<sub>2</sub> and a hypoxia culture chamber to decide which is the most advantageous model. Also, compare the metabolic profiles.
- To verify the role of ROS scavenging in angiogenesis, in order to determine if an anti-ROS therapeutic strategy would be worthy to test in order to disturb angiogenesis.
- To study in depth the propranolol mechanism of action in angiogenesis inhibition, in order to determine whether  $\beta_1$  or  $\beta_2$  adrenergic receptors are involved and which signaling pathways can be further activated in this inhibitory process.
- To test the effect of propranolol *in vivo* using a plug assay with HUVECs and in cancer murine xenograft models to unravel the role in tumor neo-vasculature.
- Testing nanoparticles loaded with  $\beta$ -blockers targeting endothelial cells (*in vitro* and *in vivo*).

## 6. References

1. Latest global cancer data : Cancer burden rises to 18.1 million new cases and 9.6 million cancer deaths in 2018. *World Health Organization*
2. Lodish, H. *et al. Molecular Cell Biology*. (W. H. Freeman and Company, 2016).
3. Alberts, B. *et al. Molecular Biology of the Cell*. (Garland Science, 2008).
4. Hemminki, A. & Hemminki, K. The Genetic Basis of cancer. in *Cancer Gene Therapy* 9–18 (2005). doi:10.1007/978-1-59745-458-2\_5
5. Goldberg, A. D., Allis, C. D. & Bernstein, E. Epigenetics: A Landscape Takes Shape. *Cell* **128**, 635–638 (2007).
6. Bock, K. De, Mazzone, M. & Carmeliet, P. Antiangiogenic therapy , hypoxia , and metastasis : risky liaisons , or not ? *Nat. Rev. Clin. Oncol.* **8**, 393–404 (2011).
7. Serpa, J. & Dias, S. Metabolic cues from the microenvironment act as a major selective factor for cancer progression and metastases formation. *Cell Cycle* **10**, 180–181 (2011).
8. Hanahan, D. & Weinberg, R. A. The Hallmarks of Cancer. *Cell* **100**, 57–70 (2000).
9. Hanahan, D. & Weinberg, R. A. Hallmarks of Cancer: The Next Generation. *Cell* **144**, 646–674 (2011).
10. Domingues, G., Fernandes, S. G. & Serpa, J. Dynamics of VEGF-A and its Receptors in Cancer Vascularization – An Overview. in
11. Eelen, G. *et al. Endothelial Cell Metabolism. Physiol. Rev.* **98**, 3–58 (2018).
12. Jung, S. & Kleinheinz, J. Angiogenesis - The Key to Regeneration. in *Regenerative Medicine and Tissue Engineering* 453–473 (IntechOpen, 2013).
13. Sliwinska, P. N. *et al. Consensus guidelines for the use and interpretation of angiogenesis assays. Springer* (2018).

14. Stacker, S. A. & Achen, M. G. The VEGF signaling pathway in cancer: The road ahead. *Chin. J. Cancer* **32**, 297–302 (2013).
15. Kowanetz, M. Vascular Endothelial Growth Factor Signaling Pathways: Therapeutic Perspective. *Clin. Cancer Res.* **12**, 5018–5022 (2006).
16. Blanco, R. & Gerhardt, H. VEGF and Notch in Tip and Stalk Cell Selection. *Cold Spring Harb. Perspect. Med.* 1–19 (2013).
17. Wong, B. W., Marsch, E., Treps, L., Baes, M. & Carmeliet, P. Endothelial cell metabolism in health and disease : impact of hypoxia. *EMBO J.* 1–17 (2017). doi:10.15252/embj.201696150
18. Zecchin, A., Kalucka, J., Dubois, C. & Carmeliet, P. How endothelial Cells Adapt Their Metabolism to Form Vessels in Tumors. *Front. Immunol.* **8**, (2017).
19. Potente, M., Gerhardt, H. & Carmeliet, P. Basic and Therapeutic Aspects of Angiogenesis. *Cell* **146**, 873–887 (2011).
20. Folkman, J. Tumor Angiogenesis: Therapeutic Implications. *N. Engl. J. Med.* **285**, 1182–1186 (1971).
21. Gimbrone, M. A., Leapman, S. B., Cotran, R. S. & Folkman, J. Tumor Dormancy in vivo by Prevention of neovascularization. *J. Exp. Med.* **136**, 261–276 (1972).
22. Rohlenova, K., Veys, K., Miranda-Santos, I., Bock, K. De & Carmeliet, P. Endothelial Cell Metabolism in Health and Disease. *Trends Cell Biol.* 1–13 (2017). doi:10.1016/j.tcb.2017.10.010
23. Verdegem, D., Moens, S., Stapor, P. & Carmeliet, P. Endothelial cell metabolism : parallels and divergences with cancer cell metabolism. *Cancer Metab.* **2**, 1–19 (2014).
24. Draoui, N., Zeeuw, P. De & Carmeliet, P. Angiogenesis revisited from a metabolic perspective : role and therapeutic implications of endothelial cell metabolism. (2017).
25. Pavlova, N. N. & Thompson, C. B. The Emerging Hallmarks of Cancer Metabolism. *Cell Metab.* **23**, 27–47 (2017).
26. Hsu, P. P. & Sabatini, D. M. Cancer cell metabolism: Warburg and beyond. *Cell* **134**, 703–707 (2008).
27. GUPPY, M., LEEDMAN, P., ZU, X. & RUSSELL, V. Contribution by different fuels and metabolic pathways to the total ATP turnover of proliferating MCF-7 breast cancer cells. *Biochem. J.* **364**, 309–315 (2002).
28. Alam, M. M., Lal, S., FitzGerald, K. E. & Zhang, L. A holistic view of cancer bioenergetics: mitochondrial function and respiration play fundamental roles in the development and progression of diverse tumors. *Clin. Transl. Med.* **5**, (2016).
29. Rodríguez-Enríquez, S., Torres-Márquez, M. E. & Moreno-Sánchez, R. Substrate oxidation and ATP supply in AS-30D hepatoma cells. *Arch. Biochem. Biophys.* **375**, 21–30 (2000).
30. Rodríguez-Enríquez, S. *et al.* Control of cellular proliferation by modulation of oxidative phosphorylation in human and rodent fast-growing tumor cells. *Toxicol. Appl. Pharmacol.* **215**, 208–217 (2006).
31. Hensley, C. T., Wasti, A. T. & DeBerardinis, R. J. Glutamine and cancer: cell biology, physiology, and clinical opportunities. *J. Clin. Invest.* **123**, 3678–3684 (2013).
32. Villalba, M. *et al.* From tumor cell metabolism to tumor immune escape. *Int. J. Biochem. Cell Biol.* **45**, 106–113 (2013).
33. Currie, E., Schulze, A., Zechner, R., Walther, T. C. & Farese, R. V. Cellular Fatty Acid Metabolism and Cancer. *Cell Metab.* **18**, 153–161 (2013).

34. Lo, M., Wang, Y. Z. & Gout, P. W. The xc- cystine/glutamate antiporter: A potential target for therapy of cancer and other diseases. *J. Cell. Physiol.* **215**, 593–602 (2008).
35. Bannai, S. & Kitamura, E. Transport Interaction. *J. Biol. Chem.* **265**, 2372–2376 (1980).
36. Griffith, O. W. Biologic and pharmacologic regulation of mammalian glutathione synthesis. *Free Radic. Biol. Med.* **27**, 922–935 (1999).
37. Liou, G.-Y. & Storz, P. Reactive oxygen species in cancer. *Free Radic. Res.* **44**, 479–496 (2010).
38. Vučetić, M., Cormerais, Y., Parks, S. K. & Pouyssegur, J. The Central Role of Amino Acids in Cancer Redox Homeostasis: Vulnerability Points of the Cancer Redox Code. *Front. Oncol.* **7**, (2017).
39. Munir, R., Lisec, J., Swinnen, J. V. & Zaidi, N. Lipid metabolism in cancer cells under metabolic stress. *Br. J. Cancer* **120**, 1090–1098 (2019).
40. Yan, S. Long-chain acyl-CoA synthetase in fatty acid metabolism involved in liver and other diseases: An update. *World J. Gastroenterol.* **21**, 3492 (2015).
41. Whiteside, T. The tumor microenvironment and its role in promoting tumor growth. *Oncogene* **27**, 5904–5912 (2008).
42. Lopes-Coelho, F., Gouveia-Fernandes, S. & Serpa, J. Metabolic cooperation between cancer and non-cancerous stromal cells is pivotal in cancer progression. *Tumor Biol.* **40**, 1–15 (2018).
43. Lopes-Coelho, F., Gouveia-Fernandes, S., Nunes, S. C. & Serpa, J. Metabolic Dynamics in Breast Cancer: Cooperation between Cancer and Stromal Cells. *J. Clin. Breast Cancer Res.* **1**, 1–7 (2017).
44. Lyssiotis, C. A. & Kimmelman, A. C. Metabolic Interactions in the Tumor Microenvironment. *Trends Cell Biol.* **27**, 863–875 (2017).
45. Lopes-Coelho, F., Martins, F. & Serpa, J. Endothelial cells (ECs) metabolism: a valuable piece to disentangle cancer biology. in *Tumor Microenvironment - The main driver of metabolic adaptation* (Springer Nature, 2019).
46. de Alteriis, E., Carteni, F., Parascandola, P., Serpa, J. & Mazzoleni, S. Revisiting the Crabtree/Warburg effect in a dynamic perspective: a fitness advantage against sugar-induced cell death. *Cell Cycle* **17**, 688–701 (2018).
47. Bock, K. De, Georgiadou, M. & Carmeliet, P. Role of Endothelial Cell Metabolism in Vessel Sprouting. *Cell Metab.* **18**, 634–647 (2013).
48. Yang, S., Yin, J. & Hou, X. Inhibition of miR-135b by SP-1 promotes hypoxia- induced vascular endothelial cell injury via HIF-1 $\alpha$ . *Exp. Cell Res.* (2018). doi:10.1016/j.yexcr.2018.06.001
49. Semenza, G. L. Defining the Role of Hypoxia-Inducible Factor 1 in Cancer Biology and Therapeutics. *Oncogene* **29**, 625–634 (2010).
50. Takiyama, Y. & Haneda, M. Hypoxia in Diabetic Kidneys. *Biomed Res. Int.* (2014). doi:10.1155/2014/837421
51. Petrova, V., Annicchiarico-petruzzelli, M., Melino, G. & Amelio, I. The hypoxic tumour microenvironment. *Oncogenesis* **7**, (2018).
52. Sen Banerjee, S. *et al.* HIF–prolyl hydroxylases and cardiovascular diseases. *Toxicol. Mech. Methods* **22**, 347–358 (2012).
53. Nunes, S. C. *et al.* Cysteine boosts the evolutionary adaptation to CoCl<sub>2</sub> mimicked hypoxia conditions, favouring carboplatin resistance in ovarian cancer. *BMC Evol. Biol.* **18**, 1–17 (2018).

54. Nunes, S. C. *et al.* Cysteine allows ovarian cancer cells to adapt to hypoxia and to escape from carboplatin cytotoxicity. *Sci. Rep.* **8**, 1–17 (2018).
55. Wu, D. *et al.* Hydrogen sulfide in cancer: Friend or foe? *Nitric Oxide* **50**, 38–45 (2015).
56. Hellmich, M. R. & Szabo, C. Hydrogen Sulfide and Cancer. in **230**, 233–241 (2015).
57. Bang, I. & Choi, H. Structural Features of  $\beta_2$  Adrenergic Receptor: Crystal Structures and Beyond. *Mol. Cells* **38**, 105–111 (2015).
58. Kulik, G. ADRB2-Targeting Therapies for Prostate Cancer. *Cancers (Basel)*. **11**, 358 (2019).
59. Johnson, M. Molecular mechanisms of  $\beta_2$ -adrenergic receptor function, response, and regulation. *J. Allergy Clin. Immunol.* **117**, 18–24 (2006).
60. Kum, J. J. Y. & Khan, Z. A. Mechanisms of propranolol action in infantile hemangioma. *Dermatoendocrinol.* **6**, 1–7 (2014).
61. Wachter, S. B. & Gilbert, E. M. Beta-Adrenergic Receptors, from Their Discovery and Characterization through Their Manipulation to Beneficial Clinical Application. *Cardiology* **122**, 104–112 (2012).
62. Al-Majed, A. A., Bakheit, A. H. H., Abdel Aziz, H. A., Alajmi, F. M. & AlRabiah, H. Propranolol. in *Profiles of Drug Substances, Excipients, and Related Methodology* **42**, 287–338 (2017).
63. Escarcega González, C. E., González Hernández, A., Villalón, C. M., Rodríguez, M. G. & Marichal Cancino, B. A.  $\beta$ -Adrenoceptor Blockade for Infantile Hemangioma Therapy: Do  $\beta_3$ -Adrenoceptors Play a Role? *J. Vasc. Res.* **55**, 159–168 (2018).
64. Storch, C. H. & Hoeger, P. H. Propranolol for infantile haemangiomas: insights into the molecular mechanisms of action. *Br. J. Dermatol.* **163**, 269–274 (2010).
65. Rotter, A. & de Oliveira, Z. N. P. Infantile hemangioma: pathogenesis and mechanisms of action of propranolol. *JDDG J. der Dtsch. Dermatologischen Gesellschaft* **15**, 1185–1190 (2017).
66. Markley, J. L. *et al.* The future of NMR-based metabolomics. *Curr. Opin. Biotechnol.* **43**, 34–40 (2017).
67. Emwas, A.-H. *et al.* NMR Spectroscopy for Metabolomics Research. *Metabolites* **9**, 123 (2019).
68. Brown, R. M., Meah, C. J., Heath, V. L., Styles, I. B. & Bicknell, R. Tube-Forming Assays. in *Angiogenesis Protocols* **1430**, 149–157 (2016).
69. Decicco-Skinner, K. L. *et al.* Endothelial Cell Tube Formation Assay for the In Vitro Study of Angiogenesis. *J. Vis. Exp.* 1–8 (2014). doi:10.3791/51312
70. Grada, A., Otero-vinas, M., Prieto-castrillo, F., Obagi, Z. & Falanga, V. Research Techniques Made Simple : Analysis of Collective Cell Migration Using the Wound Healing Assay. *J. Invest. Dermatol.* **137**, e11–e16 (2017).
71. Sherman, H. & Rothenberg, M. Cell Migration , Chemotaxis and Invasion Assay Using Staining Protocol. *Corning* (2012).
72. Jiang, L. *et al.* Monitoring the progression of cell death and the disassembly of dying cells by flow cytometry. *Nat. Protoc.* **11**, 655–663 (2016).
73. Riccardi, C. & Nicoletti, I. Analysis of apoptosis by propidium iodide staining and flow cytometry. *Nat. Protoc.* **1**, 1458–1461 (2006).
74. Odell, I. D. & Cook, D. Immunofluorescence Techniques. *J. Invest. Dermatol.* **133**, 1–4 (2013).
75. Goodwin, A. M. In vitro assays of angiogenesis for assessment of angiogenic and anti-angiogenic

- agents. *Microvasc. Res.* **74**, 172–183 (2009).
76. Baker, M. *et al.* Use of the mouse aortic ring assay to study angiogenesis. *Nat. Protoc.* **7**, 89–104 (2011).
  77. Aplin, A. C. & Nicosia, R. F. The Aortic Ring Assay and Its Use for the Study of Tumor. in *Tumor Angiogenesis Assays: Methods and Protocols* **1464**, 63–72 (2016).
  78. van Buul, J. D. *et al.* ICAM-1 Clustering on Endothelial Cells Recruits VCAM-1. *J. Biomed. Biotechnol.* **2010**, 1–9 (2010).
  79. Lawson, C. & Wolf, S. ICAM-1 signaling in endothelial cells. *Pharmacol. Reports* **61**, 22–32 (2009).
  80. van Buul, J. D., Kanters, E. & Hordijk, P. L. Endothelial Signaling by Ig-Like Cell Adhesion Molecules. *Arterioscler. Thromb. Vasc. Biol.* **27**, 1870–1876 (2007).
  81. Wang, Z. & Yan, X. CD146, a multi-functional molecule beyond adhesion. *Cancer Lett.* **330**, 150–162 (2013).
  82. Randi, A. M. & Laffan, M. A. Von Willebrand factor and angiogenesis: basic and applied issues. *J. Thromb. Haemost.* **15**, 13–20 (2017).
  83. Watnick, R. S. The Role of the Tumor Microenvironment in Regulating Angiogenesis. *Cold Spring Harb. Perspect. Med.* **2**, 1–20 (2012).
  84. Eelen, G., Zeeuw, P. de, Simons, M. & Carmeliet, P. Endothelial cell metabolism in normal and diseased vasculature. *Circ. Res.* **116**, 1231–1244 (2015).
  85. Ghesquière, B., Wong, B. W., Kuchnio, A. & Carmeliet, P. Metabolism of stromal and immune cells in health and disease. *Nature* **511**, 167–176 (2014).
  86. Wang, D. *et al.* Hypoxia induces lactate secretion and glycolytic efflux by downregulating mitochondrial pyruvate carrier levels in human umbilical vein endothelial cells. *Mol. Med. Rep.* **18**, 1710–1717 (2018).
  87. Diaz, S. O. *et al.* Metabolic Biomarkers of Prenatal Disorders: An Exploratory NMR Metabonomics Study of Second Trimester Maternal Urine and Blood Plasma. *J. Proteome Res.* **10**, 3732–3742 (2011).
  88. Pietzke, M., Meiser, J. & Vazquez, A. Formate metabolism in health and disease. *Mol. Metab.* 1–15 (2019). doi:10.1016/j.molmet.2019.05.012
  89. Ghaly, A. E. & Kok, R. The effect of sodium sulfite and cobalt chloride on the oxygen transfer coefficient. *Appl. Biochem. Biotechnol.* **19**, 259–270 (1988).
  90. Muñoz-Sánchez, J. & Chánez-Cárdenas, M. E. The use of cobalt chloride as a chemical hypoxia model. *J. Appl. Toxicol.* 1–15 (2018). doi:10.1002/jat.3749
  91. Epstein, A. C. R. *et al.* C. elegans EGL-9 and Mammalian Homologs Define a Family of Dioxygenases that Regulate HIF by Prolyl Hydroxylation. *Cell* **107**, 43–54 (2001).
  92. Wu, D. & Yotnda, P. Induction and Testing of Hypoxia in Cell Culture. *J. Vis. Exp.* 4–7 (2011). doi:10.3791/2899
  93. Goldberg, M. A., Dunning, S. P. & Bunn, H. F. Regulation of the erythropoietin gene: evidence that the oxygen sensor is a heme protein. *Science (80-. ).* **242**, 1412–5 (1998).
  94. Al Okail, M. S. Cobalt chloride, a chemical inducer of hypoxia-inducible factor-1 $\alpha$  in U251 human glioblastoma cell line. *J. Saudi Chem. Soc.* **14**, 197–201 (2010).
  95. Yuan, Y., Hilliard, G., Ferguson, T. & Millhorn, D. E. Cobalt Inhibits the Interaction between

- Hypoxia-inducible Factor- $\alpha$  and von Hippel-Lindau Protein by Direct Binding to Hypoxia-inducible Factor- $\alpha$ . *J. Biol. Chem.* **278**, 15911–15916 (2003).
96. Vengellur, A., Phillips, J. M., Hogenesch, J. B. & Lapres, J. J. Gene expression profiling of hypoxia signaling in human hepatocellular carcinoma cells. *Physiol Genomics* **22**, 308–318 (2005).
  97. Chandel, N. S. *et al.* Mitochondrial reactive oxygen species trigger hypoxia-induced transcription. *Proc. Natl. Acad. Sci.* **95**, 11715–11720 (1998).
  98. Aplin, A. C. & Nicosia, R. F. Hypoxia paradoxically inhibits the angiogenic response of isolated vessel explants while inducing overexpression of vascular endothelial growth factor. *Angiogenesis* **19**, 133–146 (2016).
  99. Couto, N., Wood, J. & Barber, J. The role of glutathione reductase and related enzymes on cellular redox homeostasis network. *Free Radic. Biol. Med.* **95**, 27–42 (2016).
  100. Prasai, P. K., Shrestha, B., Orr, A. W. & Pattillo, C. B. Decreases in GSH:GSSG activate vascular endothelial growth factor receptor 2 (VEGFR2) in human aortic endothelial cells. *Redox Biol.* **19**, 22–27 (2018).
  101. Magdalena Radomska-Leśniewska, D., Bałan, B. J. & Skopiński, P. Angiogenesis modulation by exogenous antioxidants. *Cent. Eur. J. Immunol.* **42**, 370–376 (2017).
  102. Kubota, M. *et al.* Hydrogen and N -Acetyl- l -Cysteine Rescue Oxidative Stress-Induced Angiogenesis in a Mouse Corneal Alkali-Burn Model. *Investig. Ophthalmology Vis. Sci.* **52**, 427–433 (2011).
  103. Agarwal, A., Muñoz-Nájjar, U., Klueh, U., Shih, S.-C. & Claffey, K. P. N-Acetyl-Cysteine Promotes Angiostatin Production and Vascular Collapse in an Orthotopic Model of Breast Cancer. *Am. J. Pathol.* **164**, 1683–1696 (2004).
  104. Léauté-Labrèze, C. *et al.* Propranolol for Severe Hemangiomas of Infancy. *N. Engl. J. Med.* **358**, 2649–2651 (2008).
  105. Lamy, S., Lachambre, M.-P., Lord-Dufour, S. & Béliveau, R. Propranolol suppresses angiogenesis in vitro: Inhibition of proliferation, migration, and differentiation of endothelial cells. *Vascul. Pharmacol.* **53**, 200–208 (2010).
  106. Zhenyukh, O. *et al.* Branched-chain amino acids promote endothelial dysfunction through increased reactive oxygen species generation and inflammation. *J. Cell. Mol. Med.* **22**, 4948–4962 (2018).
  107. Cantelmo, A. R. *et al.* Inhibition of the Glycolytic Activator PFKFB3 in Endothelium Induces Tumor Vessel Normalization, Impairs Metastasis, and Improves Chemotherapy. *Cancer Cell* **30**, 968–985 (2016).

## 7. Appendices

Solutions prepared during the experimental work:

### **10X PBS (pH 7.4-7.6)**

For 1 L:

80g NaCl (1.37M) (106404, Merck)  
2g KH<sub>2</sub>PO<sub>4</sub> (14.7mM) (104873, Merck)  
11.1g Na<sub>2</sub>HPO<sub>4</sub> (78.1mM) (S-0876, Sigma)  
2g KCl (26.8mM) (104936, Merck)  
ddH<sub>2</sub>O to 1L

### **50 µg/mL Propidium Iodide (PI) solution**

For 50 mL:

1 mL of 2.5 mg/mL PI solution (P4170, Sigma) (prepared in 1X PBS)  
49 mL 1X PBS

### **Annexin binding buffer 1X**

0.01 M Hepes (pH 7.4) (391333, Millipore)  
0.14 M NaCl (106404, Merck)  
2.5 mM CaCl<sub>2</sub> (449709, Sigma)

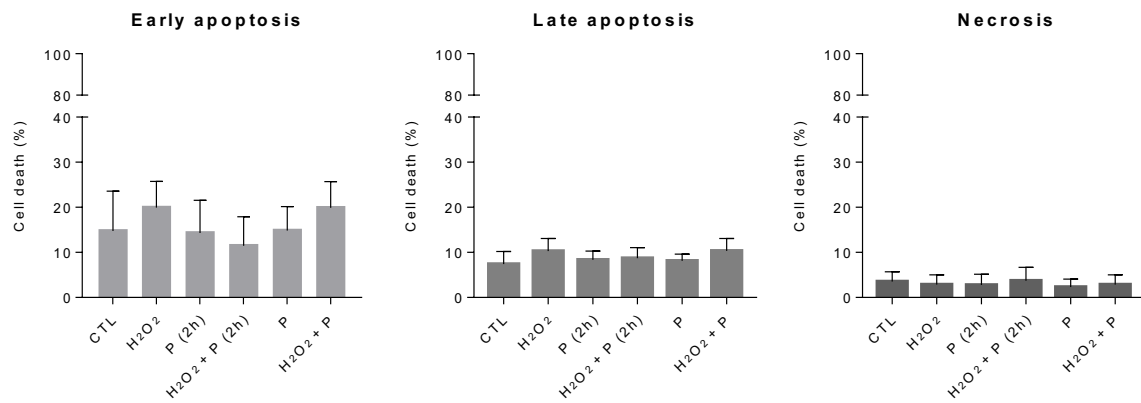
### **PBS 0.1% (w/v) BSA**

0.1g BSA (A9647, Sigma)  
100 mL 1X PBS

### **Crystal violet staining solution**

For 100 mL:

10 mL of a crystal violet solution 5%  
25 mL methanol  
65 mL ddH<sub>2</sub>O



**Supplementary Figure 1 – Propranolol don't affect cell viability.** Cells were exposed for 6h to H<sub>2</sub>O<sub>2</sub>, Propranolol (for the last 2h and for the whole 6h) with or without H<sub>2</sub>O<sub>2</sub>. Results are shown as mean  $\pm$  SD. No statistical differences were observed in early, late apoptosis or necrosis between treatments.